

Spring 5-31-2016

## Development and analysis of aluminum-PTFE reactive composite material

Siva Kumar Valluri  
*New Jersey Institute of Technology*

Follow this and additional works at: <https://digitalcommons.njit.edu/theses>



Part of the [Chemical Engineering Commons](#)

---

### Recommended Citation

Valluri, Siva Kumar, "Development and analysis of aluminum-PTFE reactive composite material" (2016).  
*Theses*. 281.  
<https://digitalcommons.njit.edu/theses/281>

This Thesis is brought to you for free and open access by the Electronic Theses and Dissertations at Digital Commons @ NJIT. It has been accepted for inclusion in Theses by an authorized administrator of Digital Commons @ NJIT. For more information, please contact [digitalcommons@njit.edu](mailto:digitalcommons@njit.edu).

## **Copyright Warning & Restrictions**

The copyright law of the United States (Title 17, United States Code) governs the making of photocopies or other reproductions of copyrighted material.

Under certain conditions specified in the law, libraries and archives are authorized to furnish a photocopy or other reproduction. One of these specified conditions is that the photocopy or reproduction is not to be “used for any purpose other than private study, scholarship, or research.” If a user makes a request for, or later uses, a photocopy or reproduction for purposes in excess of “fair use” that user may be liable for copyright infringement,

This institution reserves the right to refuse to accept a copying order if, in its judgment, fulfillment of the order would involve violation of copyright law.

**Please Note: The author retains the copyright while the New Jersey Institute of Technology reserves the right to distribute this thesis or dissertation**

Printing note: If you do not wish to print this page, then select “Pages from: first page # to: last page #” on the print dialog screen

The Van Houten library has removed some of the personal information and all signatures from the approval page and biographical sketches of theses and dissertations in order to protect the identity of NJIT graduates and faculty.

## **ABSTRACT**

### **DEVELOPMENT AND ANALYSIS OF ALUMINUM-PTFE REACTIVE COMPOSITE MATERIAL**

**by  
Siva Kumar Valluri**

The shortcomings of micron sized aluminum due to the oxide barrier and two phase losses pose a hindrance for its efficient use as a fuel. In this study a fluoropolymer; Teflon's inclusion in micron sized -325 mesh aluminum is suggested as a replacement to aluminum. Aluminum Teflon based energetic material see great potential for use in pyrotechnics, propellants and even explosives. A composite with composition Al-PTFE (90-10 wt. %) is prepared through Cryomilling and is shown to be a better method of preparation as compared to room temperature milling. The prepared materials are studied to identify best conditions. The analysis methods include thermal studies both aerobic and anaerobic, Mass Spectrometry, XRD analysis and ESD experiments. The best materials are shown to retain the Teflon till higher temperatures as compared with other materials such as nano powder mixtures and milled composites of Al-PTFE, both of composition (70-30 wt. %). The milled material exhibits two exothermic peaks at 405.4°C and 540°C which correspond to the phenomena of fluorine's interaction with the oxide to form aluminum fluoride and the phase transition into a more stable fluoride of aluminum respectively. The activation energy for these reactions are on the higher side at 145.8 and 266.4 kJ/mol. This study offers a better milling process to make more reactive composites of micron sized Al and granular Teflon (PTFE).

**DEVELOPMENT AND ANALYSIS OF  
ALUMINUM-PTFE REACTIVE COMPOSITE MATERIAL**

by  
**Siva Kumar Valluri**

**A Thesis  
Submitted to the Faculty of  
New Jersey Institute of Technology  
in Partial Fulfillment of the Requirements for the Degree of  
Master of Science in Chemical Engineering**

**Otto H. York Department of  
Chemical, Biological and Pharmaceutical Engineering**

**May 2016**

Blank Page

**APPROVAL PAGE**

**DEVELOPMENT AND ANALYSIS OF  
ALUMINUM-TEFLON ENERGETIC COMPOSITE**

**Siva Kumar Valluri**

---

Dr. Edward L. Dreizin, Dissertation Advisor  
Professor of Chemical Engineering, NJIT

Date

---

Dr. Reginald P. Tomkins, Committee Member  
Professor of Chemical Engineering, NJIT

Date

---

Dr. Mirko Schoenitz, Committee Member  
Associate Research Professor of Chemical Engineering, NJIT

Date

## **BIOGRAPHICAL SKETCH**

**Author:** Siva Kumar Valluri

**Degree:** Master of Science

**Date:** May 2016

### **Undergraduate and Graduate Education:**

- Master of Science in Chemical Engineering,  
New Jersey Institute of Technology, Newark, NJ, 2016
- Master of Science in Chemistry,  
Birla Institute of Technology and Sciences-Pilani, Hyderabad, India, 2014
- Bachelor of Science in Chemical Engineering,  
Birla Institute of Technology and Sciences-Pilani, Hyderabad, India, 2014

**Major:** Chemical Engineering



This thesis is dedicated to all of my loved ones;  
grandparents, parents and my brother, Chaitanya.

నా లేనిదే నేను లేను

(Without mine, there is no me)

## ACKNOWLEDGMENT

I would like to take this opportunity to thank all the people who have been instrumental in making me who I am today. I shall remember them every day, every hour. Here are some wonderful people without whose help, this project would not have been possible.

It is with great admiration and respect that I acknowledge the support of Dr. Edward Dreizin throughout my graduate study. His mammoth contribution to the field never ceases to inspire and motivate me. I would like to thank him for taking an active interest in all the details of my work and helping me direct my thoughts to appropriate practices. All the care and concern he's shown shan't be forgot.

I would like to acknowledge my committee members Dr. Reginald Tomkins and Dr. Mirko Schoenitz. I thank Dr. Tomkin's for being ever so approachable and helpful. Dr. Mirko's characteristic humor and creative approach to solve problems turned mountains to molehills. He has taught me never to shy away from going all the way through to answer one's curiosity.

I would like to thank my fellow lab mates for their help and guidance through my research. They've always had my back through highs and especially the lows. Their friendship made tedious work hours more enjoyable.

All of this would be for naught if not for the support and love of my parents, brother, teachers and friends. This is but a small labor of love to all of these backstage crew.

## TABLE OF CONTENTS

<b>Chapter</b>	<b>Page</b>
1 INTRODUCTION.....	1
1.1 Background.....	1
2 EXPERIMENTAL.....	5
2.1 Materials.....	5
2.2 Milling Devices and Respective Conditions.....	6
2.3 Characterization of Prepared Material.....	8
3 RESULTS.....	11
3.1 Observation.....	11
3.1.1 Milled Material.....	11
3.1.2 Thermal Analysis and Mass Spectroscopy.....	14
3.1.3 XRD Analysis.....	23
3.1.4 ESD Experiment.....	28
3.2 Discussion.....	31
3.2.1 Best Performing Material.....	31
3.2.2 Comparison with other Al-PTFE Preparations.....	31
4 CONCLUSIONS.....	35
5 REFERENCES.....	38

## LIST OF TABLES

<b>Table</b>		<b>Page</b>
2.1	All Al-PTFE (90-10 wt. %) Milled Sample ID and their Conditions.....	6
2.2	Parameters of the Shaker and Attritor Mills to Achieve Equivalent Milling Progress as Measured by their Milling Dose as Established by (Santhanam, 2012).....	7

## LIST OF FIGURES

<b>Figure</b>	<b>Page</b>
2.1 Volumetric and corresponding gravimetric composition of aluminum in Al-PTFE study.....	5
2.2 Schematic diagram of the ESD ignition experiment.....	10
3.1 SEM images at 2K magnification for Al-PTFE (90-10 wt. %) samples; (1) SM-2; 2-hour Shaker milled at room temperature, (2) AM-6; 6-hour Attritor milled at room temperature, (3) CM-6; 6-hour Attritor milled at cryogenic temperature, (4) CM-8.5; 8.5-hour Attritor milled at cryogenic temperature.....	12
3.2 SEM image of Al-PTFE (90-10 wt. %) AM-6 sample; room temperature attritor milled sample showing fibrous formations in the sample.....	13
3.3 SEM image of AM-6 sample; Al-PTFE (90-10 wt. %) attritor milled for 6-hour at room temperature (Left) and EDS elemental mapping of Aluminum and Fluorine (Right).....	13
3.4 SEM image of CM-6 sample; Al-PTFE (90-10 wt. %) attritor milled for 6-hour at cryogenic temperature (Left) and EDS elemental mapping of Aluminum and Fluorine (Right).....	14
3.5 TG plots of all Al-PTFE (90-10 wt. %) milled material in anaerobic environment (100ml/min argon) in a temperature range of 30°C-1000°C with a heating rate of 20K/min.....	15
3.6 DTA plots of all Al-PTFE (90-10 wt. %) milled material in anaerobic environment (100ml/min of argon) in a temperature range of 30°C-775°C with a heating rate of 20K/min.....	16
3.7 DTA plots in anaerobic environment (100ml/min of argon) in a temperature range of 250°C-700°C with various heating rates (5K/min, 10K/min, 20K/min) of CM-6; 6-hour cryogenic attritor milled Al-PTFE (90-10 wt. %) milled material.....	18
3.8 Kissinger plots for the two minor exotherms observed in the temperature range of 350°C-600°C with various heating rates (5K/min, 10K/min, 20K/min) of CM-6; 6-hour cryogenic attritor milled Al-PTFE (90-10 wt. %) milled material..	18

**LIST OF FIGURES**  
**(Continued)**

<b>Figure</b>	<b>Page</b>
3.9 TG plots of all Al-PTFE (90-10 wt. %) milled material in aerobic environment (100ml/min of oxygen and argon; 50-50 v/v) in a temperature range of 30°C-1000°C with a heating rate of 5K/min.....	19
3.10 DTA plots of all Al-PTFE (90-10 wt. %) milled material in aerobic environment (100ml/min of oxygen and argon; 50-50 v/v) in a temperature range of 30°C-1000°C with a heating rate of 5K/min.....	22
3.11 Preliminary Study with XRD patterns of Al-PTFE (95-5 wt. %) shaker milled material and quenched samples in anaerobic environment (100ml/min of argon).....	23
3.12 XRD patterns of freshly prepared of Al-PTFE (90-10 wt. %) composition for comparable samples prepared by milling in shaker mill for 2-hour and attritor mill at room temperatures and cryogenic temperatures for 6-hour milling periods.....	24
3.13 XRD patterns of Al-PTFE (90-10 wt. %) attritor mill samples prepared at cryogenic temperatures for various milling periods (1.5-hour, 6-hour, 8.5-hour).....	25
3.14 XRD patterns of Al-PTFE (90-10 wt. %) attritor mill samples prepared at cryogenic temperatures for various milling periods (1.5-hour and 6-hour) and their respective samples after their first weight loss in oxidative thermal analysis.....	26
3.15 XRD patterns of Al-PTFE (90-10 wt. %) shaker milled samples collected at various temperatures (30°C, 480°C,600°C,775°C and1000°C) and corresponding TG/DTA significance of collected samples.....	27
3.16 The Pressure plot generated in ESD (12kV, 10000pf capacitance) for 6-hour and 8.5-hour attritor milled at cryogenic temperature samples.....	29
3.17 The Light emission plot during ESD (12kV, 10000pf capacitance) for 6-hour and 8.5-hour attritor milled at cryogenic temperature samples.....	30

**LIST OF FIGURES  
(Continued)**

<b>Figure</b>	<b>Page</b>
3.18 Comparison of TG plots in anaerobic environment (20K/min, argon atmosphere) in a temperature range of 100°C-1000°C among various Al-PTFE samples; 6-hour cryogenic attritor milled Al-PTFE (90-10 wt. %) and Al-PTFE (70-30 wt. %) composition milled materials and mixtures by (Sippel et al., 2013a).....	32
3.19 Comparison in anaerobic environment (20K/min, argon atmosphere) in a temperature range of 250°C-700°C among various Al-PTFE samples; DTA plot of 6-hour cryogenic attritor milled Al-PTFE (90-10 wt. %) and DSC plots of Al-PTFE (70-30 wt. %) composition milled materials and mixtures by (Sippel et al., 2013a) and n-Al-n-PTFE (70-30 wt. %) blend by (Osborne & Pantoya, 2007).....	33

# CHAPTER 1

## INTRODUCTION

### 1.1 Background

Aluminum is a widely used ingredient in energetic composition of all types. The benefits of micron sized aluminum such as considerable energy content, relatively lower cost, and improved stability due to oxide layer among several others, see its inclusion into solid fuels for propulsion systems. However the stable oxide layer becomes a combustion barrier as it limits the reactive surface of the aluminized fuels. Due to its high stability and high melting point (~2300 K), the rate of oxidization is dependent on the diffusion through this layer. This subsequently impact the ignition temperature of the aluminum fuel making it harder for combustion to occur. The second major shortcoming is the two-phase losses caused by the agglomeration of aluminum particle melts in the nozzle exit (Sutton, 2001). The use of nano-aluminum (n-Al or ALEX) in place of micron sized aluminum has increased the reactivity of the energetic mixtures. But the large oxide content leads to decreased propellant specific impulse caused by poor mechanical strength (Orlandi, 2005), reducing the utility of nano-aluminum in propellants.

The reactivity of the micron sized aluminum powders could be altered through small inclusions of other material, even such as wax and polyethylene (Zhang, 2012). The inclusion may be chosen appropriately to reduce the shortcomings of the micron sized fuel. Very early work on oxidizers for rocket fuel by H.R. Lips show an increase in fluorine content in FLOX (a mixture of liquid oxygen and fluorine) increased combustion efficiency of aluminized fuels (Lips, 1977). The high electronegativity of fluorine has



long since been exploited to improve the reactivity of fuels. Activation of aluminum through direct chemical treatment with fluorine based activating solvents has shown improvement in reactivity of aluminum powders (Maggi, Dossi, Paravan, DeLuca, & Liljedahl, 2015). However this method was far behind nano-powders performance and has the possibility of reducing amount of reactive aluminum in the fuel. Poly-Tetrafluoroethylene (PTFE, trade name: Teflon®) is a great source of fluorine as it contains 75%/w of fluorine(Kubota, 1987). PTFE has also been used with aluminum.

This stable relatively unreactive material has also been used to make composites and mixtures with metals to result in energetic compositions. Composites like Magnesium/Teflon®/Viton (where Viton another fluorocarbon acts as the binder) containing PTFE as oxidizer have been used as decoys and flares(Koch, Hahma, Weiser, Roth, & Knapp, 2012). Due to similarity in stoichiometry of Aluminum and Magnesium (Poehlein, 2001) and the improvement in efficiency by replacing Magnesium in MTV with Alex (Cudzilo, 2001), the focus shifted to Al/PTFE compositions.

Aluminum with Polytetrafluoroethylene (PTFE or Teflon) is a fine example of versatile energetic materials. It has the potential to fit into all three categories of energetics; explosives (Dolgoborodov, 2005), propellants (Sippel, Son, & Groven, 2014) and pyrotechnics (Sippel, Son, & Groven, 2013a) . The theoretical energy density of aluminum-PTFE is calculated using REAL code by (Belov, 2004) to be extremely high at around 1100 kJ/mole (~11,600 kJ/kg). Further a study through ab initio calculations and thermos-kinetic data of reactions between the two components aluminum and PTFE have also shown to be highly exothermic by (Losada, 2009). This theoretical study by Losada & Chaudhuri (2009) show that the reactions may be simplified into three highly

exothermic global reactions where the first step; decomposition of PTFE, is speculated to be facilitated by the alumina surface.

Several studies on the effect of PTFE on the oxide coating on aluminum particles show possibilities of increased reactivity. It is shown that the nano sized aluminum powders have interactions between the oxide layer and fluorine that give rise to a pre-ignition reaction (Osborne & Pantoya, 2007). A study by (Hobosyan, Kirakosyan, Kharatyan, & Martirosyan, 2014) shows that at higher heating rates ( $>160^{\circ}\text{C}/\text{min}$ ) the fluorinated gases effusing out of PTFE react with the alumina exothermically. They identified using isoconversional methods suggested by Starink that the activation energy for this reaction decreases from  $275\text{kJ}/\text{mol}$  at lower heating rates ( $<150^{\circ}\text{C}/\text{min}$ ) to just  $21\text{kJ}/\text{mol}$  at higher heating rates ( $>150^{\circ}\text{C}/\text{min}$ ). This is of significance as the certainty of this interaction and its ease of occurrence, paves way for improving the reactivity of aluminum powders by the removal of their ignition barrier through the use of PTFE.

It is interesting to note that the reaction between alumina and PTFE results primarily in carbon monoxide and aluminum fluoride (Hobosyan et al., 2014), a solid that sublimates at temperatures above  $1000^{\circ}\text{C}$ . This could improve the reduction in condensed particles in exit streams and thus improving specific impulse of the fuel. Another interesting consequence of milled composites of aluminum and PTFE is that they offer an alternative to aluminum which yields agglomerates upon combustion. The milled composite not only resulted in a 66% reduction in agglomerate diameter as compared to similar sized spherical aluminum powder but also a significant 55% increase in burning rate as shown by Sippel, Son, & Groven, 2013b. This holds great potential for improving aluminum's performance as a fuel in propellants and pyrotechnics through inclusions of

fluorocarbon polymers. Micron sized aluminum may be replaced by composites made from micron sized aluminum and PTFE which could improve its performance. This idea is central for this study. The mechanical properties of PTFE and aluminum powder differ drastically. The prospect of better milling through manipulation of physical form of components is of considerable importance in such a situation. This is sought through milling at cryogenic temperatures where the structural nature of granular PTFE and powdered aluminum are relatively comparable.

## CHAPTER 2

### EXPERIMENTAL

#### 2.1 Materials

In order to make a dense and metallic composite of aluminum-PTFE, PTFE is embedded into a matrix of aluminum. This is achieved by adjusting the composition to ensure volumetric dominance of the denser component; aluminum powder. From Figure 2.1 it's seen that at 85% w/w of aluminum in the mixture the volumetric presence of both substances is almost equal. For the sake of this study, analysis has been primary conducted on milled materials consisting of micron sized aluminum and granular PTFE, with 90% w/w of aluminum (60% v/v). A few runs with 95% w/w of aluminum were analyzed during the preliminary studies.

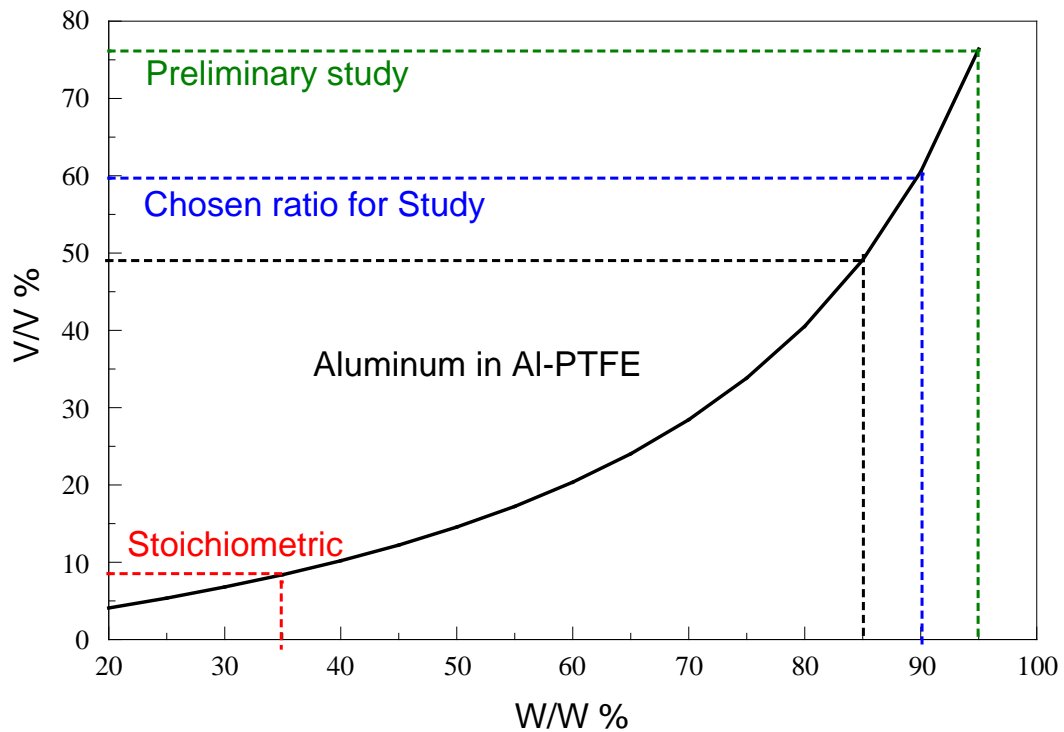


**Figure 2.1** Volumetric and corresponding gravimetric composition of aluminum in Al-PTFE study.

All of the milled material were prepared using 99% pure aluminum powder which were of the size -325 mesh supplied by Atlantic Equipment Engineers and granular Polytetrafluoroethylene (PTFE) supplied by DuPont under the name Teflon® 7A. The ratio of mixing of the two components is by weight, where 90% w/w of a batch is aluminum while the remaining 10% is PTFE. The materials used for analysis were then prepared through milling by two different equipment by primarily changing two operational conditions; the milling time and the temperature of milling vials during the milling process. The milled materials that were prepared for analysis have been listed in Table.2.1. The rationale for selecting specific milling conditions listed is discussed below. Further all the milled materials are stored in a glove box to ensure samples don't age.

**Table 2.1** All Al-PTFE (90-10 wt. %) Milled Sample ID and their Conditions

S.No	Milling Time (hours)	Shaker Milled	Milling Time (hours)	Attritor Milled	
		Room Temp		Room Temp	Cryogenic
1	0.5	SM-0.5	1.5	AM-1.5	CM-1.5
2	1	SM-1	3	AM-3	CM-3
3	2	SM-2	6	AM-6	CM-6
4			8.5		CM-8.5

## 2.2 Milling Devices and Respective Conditions

Preliminary studies have been conducted with smaller amounts of samples for two compositions Al-PTFE (95-5 wt. %) and Al-PTFE (90-10 wt. %), milled at room temperatures in the shaker mill. Later, the materials were scaled up for milling in larger quantities in the attritor mill. The scale up was based on the guidelines arrived at by the

work of (Santhanam, 2012) where the established equivalence parameters are given in Table 2.2. The equivalence has been found by equating the milling progress in equipment through the concept of milling dose ( $D_m$ ); the energy transferred to powder via tools for a given mass of powder. The milling dose  $D_m$  is expressed as a function of milling time and energy dissipation in the ball milling processes to further draw parallel between experimental and analytical calculations through Discrete Element Modeling (DEM). The equivalent milling times were extrapolated for subsequent longer periods from the basic correlation as can be seen in Table 2.1.

**Table 2.2** Parameters of the Shaker and Attritor Mills to Achieve Equivalent Milling Progress as Measured by their Milling Dose as Established by (Santhanam, 2012)

	Shaker Mill	Attritor Mill
BPR	10	36
Load (gm)	5	50
RPM	1054 (fixed)	400(fixed)
Time (hours)	0.4	1.2

Room temperature milling has been carried out in two types of milling equipment, shaker mill and attritor mill over a range of milling times. Further, the attritor mill has also been used for cryogenic milling by using liquid nitrogen as the cooling fluid. In all the milling runs, the milling media has been the same; case hardened carbon steel balls of 3/8<sup>th</sup> inch (~9.5mm) diameter. A ball to powder mass ratio (BPR) of 10 is also constant over all the runs in the shaker mill. The BPR ratio is taken to be 36 for the attritor mill throughout all of its runs irrespective of duration or temperature condition. To each of the respective milling vials, a weighed number of steel balls are added first, and then, the appropriate amounts of aluminum powder and PTFE granules were added.

The shaker mill used, is of the SPEX 8000 series and accomplishes rapid milling for relatively smaller loads (<20gms) at room temperature operation. The mill is a vibratory mill with a cyclic movement in all three dimensions. The mill is operated with pressurized air to aid cooling of the exterior surface of the sealed milling vials for three milling periods; 0.5-hour, 1-hour and 2-hour. For each of the runs a total load of 5gms of aluminum and PTFE mix (90%w/w of aluminum) was pulverized using case hardened carbon steel balls of the diameter 3/8<sup>th</sup> an inch (~9.5mm).

Composites were also prepared using the attritor mill for which a mill of model 01HD manufactured by Union Process was used. This mill has a steel impeller that rotates at a pre-designated speed and agitates the steel balls within the milling vial. The setup consists of a vial and a surrounding cooling jacket to circulate appropriate fluid of choice which is then sealed with a lid. The depth of the impeller is adjustable and is setup such that the impeller touches the bottom of the milling vial. This adjustment is made once the vial is filled with the balls and aluminum-PTFE mix and then the set-up is sealed. After sealing 99% pure nitrogen gas provided by Airgas is continuously flushed within the vial during the entirety of the milling time. The cooling fluids for room temperature milling and cryogenic milling are water and liquid nitrogen, provided by Airgas respectively. The impeller has been rotated at a speed of 400 RPM for all the different runs in the attritor mill.

### **2.3 Characterization of the Prepared Materials**

All prepared materials were examined using electron microscopy. A LEO 1530 field emission scanning electron microscope was used. The structures of materials were characterized using x-ray diffraction (XRD). XRD measurements were performed using

a PANalytical Empyrean diffractometer operated at 45 kV and 40 mA using unfiltered Cu K $\alpha$  radiation ( $\lambda = 1.5438 \text{ \AA}$ ).

Decomposition of PTFE upon heating as well as exothermic reactions occurring between aluminum and PTFE with and without the external oxidizing environment were studied using thermo-analytical measurements. A Netzsch manufactured instrument of model STA 409 was used for TGA and DTA. Samples were placed in DTA crucibles made of alumina and heated at 5K/min, 10K/min and 20K/min rates. Flow setting for which are constant at 100ml/min but the composition of gases changes for anaerobic and aerobic; 100% Argon and 50:50 Oxygen & Argon respectively. The measurements included both thermo-gravimetry (TG) and differential thermal analysis (DTA). Mass Spectrometry was run in tandem with the Netzsch equipment to identify species given out during thermal analysis. The instrument is model 5221 Extrel Core Mass Spectrometer that has been operated through Merlin Automating Data System software.

Preliminary flammability assessments were made by placing several milligrams of the prepared powder as an approximately 1-mm thick, 1-mm tall and 1-cm long strip on a piece of a porous paper (e.g., paper towel) laid on a metal wire mesh screen. The paper was ignited and it was observed whether the powder could be ignited as well. If powder ignited, its combustion was observed to detect any ejected particles and overall reaction intensity. Following these preliminary assessments, powders were ignited using an electro-static discharge. Schematic diagram of the experimental setup is shown in Figure. 2.2. Prepared powders were loaded in a 0.5-mm deep, 6-mm diameter cavity of a grounded, custom-made polished brass sample holder, which was placed in the center of a sealed chamber with a volume of 624 cm<sup>3</sup>. The excess powder was scraped away by a



razor blade to make an even layer thickness. The loaded sample holder was grounded. A high-voltage pin electrode was placed  $\sim 0.2$  mm above the surface of the powder layer. A selected capacitor in a range from 250 to 2000 pF was initially charged to a voltage in a range of 3 – 12 kV. The capacitor was then discharged through the pin electrode and the powder sample. All tests were conducted in ambient air at room temperature. The optical emission of ignited powder filtered at  $\lambda = 568$  nm was measured by a photomultiplier tube (PMT), which was placed 15 cm away from the sample. The experimental chamber was equipped with a model 482A21 dynamic pressure transducer by Piezoelectronics to record the pressure change as a function of time. A more detailed description of the experimental procedure is available elsewhere (Williams, Beloni, & Dreizin, 2012; Williams, Patel, & Dreizin, 2014).

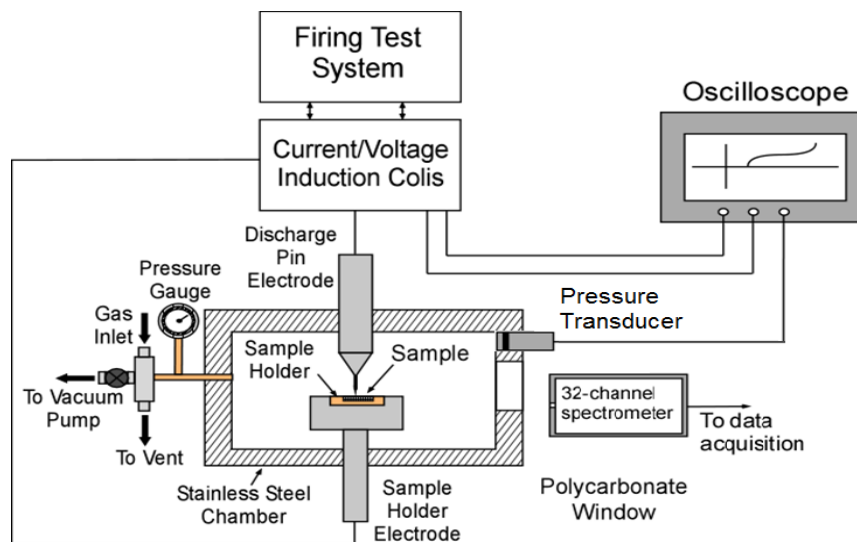


**Figure 2.2** Schematic diagram of the ESD ignition experiment.

## CHAPTER 3

### RESULTS

#### 3.1 Observations

##### 3.1.1 Milled Material

The milled materials have all been initially checked for ignition on paper. All the room temperature milled materials showed ignition while the cryogenic milled materials (CM-1.5, CM-3, CM-6 and CM-8.5) did not ignite. The ease of ignition markedly decreased with milling time for room temperature attritor milled materials. The shaker milled samples (SM-0.5, SM-1 and SM-2) ignited with greater ease than their corresponding attritor mill counterparts.

Microscopy showed that all of the room-temperature milled samples were flaky to a large extent. However, equiaxial particles were obtained after extended milling time in the attritor mill using liquid nitrogen cooling. Characteristic images of particles prepared at different milling conditions are shown in Figure. 3.1. It can be seen from Figure 3.1 that for equivalent milling periods the material yield by room temperature milling in shaker mill and attritor mill look comparable in shape and size. However the attritor milled sample appears to be slightly flakier under the SEM.

The cryogenic milling in attritor yielded smaller particles for the same milling time (compare quadrants (3) with (1) and (2) of Figure 3.1) but these particles are still flaky looking. The longest attritor milled sample in cryogenic conditions (CM-8.5) has particles that look very spheroidal and well milled as compared to lower milled material in same conditions.

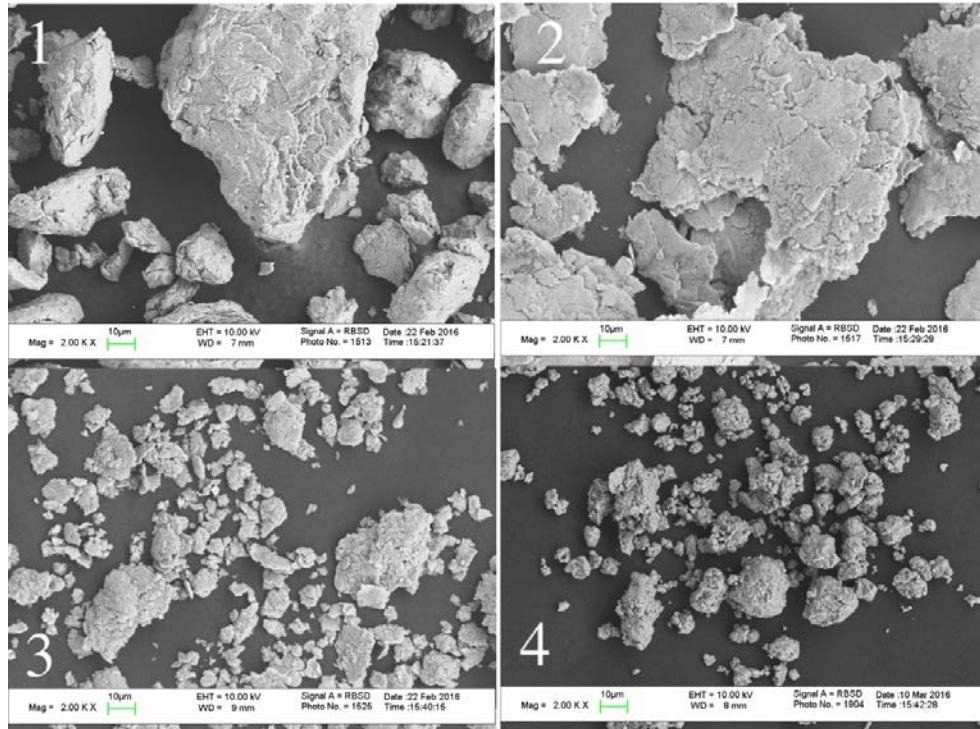


**Figure 3.1** SEM images at 2K magnification for Al-PTFE (90-10 wt. %) samples; (1) SM-2; 2-hour Shaker milled at room temperature, (2) AM-6; 6-hour Attritor milled at room temperature, (3) CM-6; 6-hour Attritor milled at cryogenic temperature, (4) CM-8.5; 8.5-hour Attritor milled at cryogenic temperature.

The samples milled at room temperature in the attritor mill show multiple fibrous formations on the surface of the particles as shown by Figure 3.2. Such structures are absent in the cryomilled samples of all milling time. The dispersion of PTFE in the aluminum matrix has been checked for attritor milled samples for 6-hour milling duration for both conditions; room temperature milling and cryogenic milling. For room temperature milling, Figure 3.3 shows the EDS elemental mapping for aluminum and fluorine which is representative of PTFE.

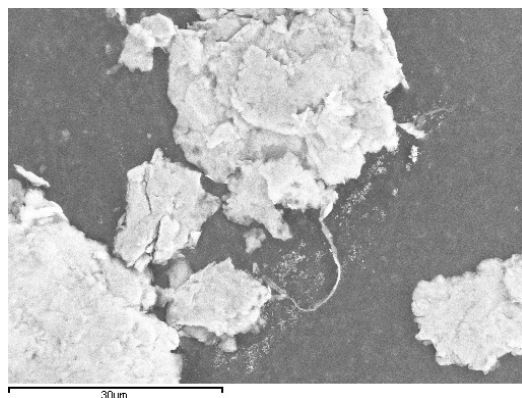


**Figure 3.2** SEM image of Al-PTFE (90-10 wt. %) AM-6 sample; room temperature attritor milled sample showing fibrous formations in the sample.

The distribution is clearly not uniform as the voids (dark spaces) in the aluminum map are filled with fluorine, based on the respective elemental map of the fluorine. This may be envisioned as PTFE being smeared non-uniformly with a majority being trapped in crevices in the particles.

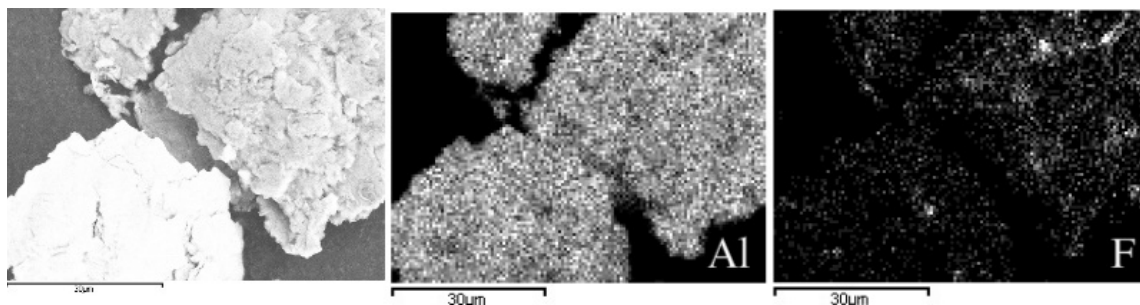


**Figure 3.3** SEM image of AM-6 sample; Al-PTFE (90-10 wt. %) attritor milled for 6hrs at room temperature (Left) and EDS elemental mapping of Aluminum and Fluorine (Right).

The material collected from cryogenic conditions CM-6 for the same milling duration of 6-hour shows homogenous dispersing of PTFE through the bulk of the particle in Figure 3.4. The density of imaging in both aluminum and fluorine elemental map follow same trends showing greater homogeneity.

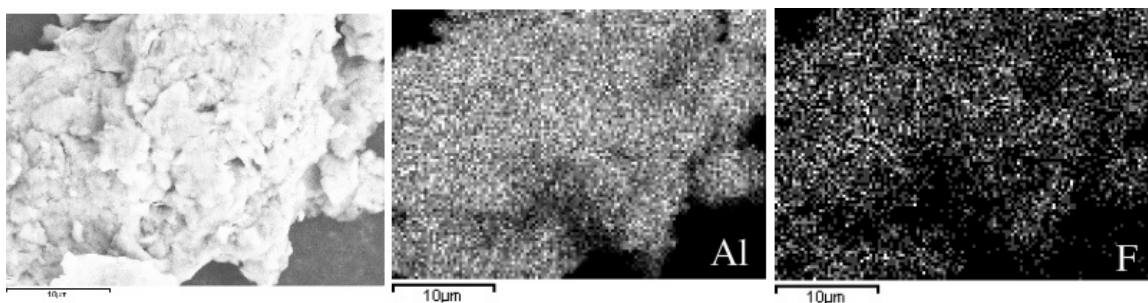


**Figure 3.4** SEM image of CM-6 sample; Al-PTFE (90-10 wt. %) attritor milled for 6-hour at cryogenic temperature (Left) and EDS elemental mapping of Aluminum and Fluorine (Right).

### 3.1.2 Thermal Analysis

The thermal analysis of the prepared material was conducted in both aerobic and anaerobic conditions where Argon was chosen as the inert flow gas. The anaerobic study was conducted in a range of 30°C-1000°C at a heating rate of 20K/min. The Figure 3.5 shows the thermogravimetric plots which capture a trend of two mass loss events. To prevent the fluorinated gases from damaging the equipment, some runs have been suspended before the second weight loss. The first mass loss occurs in temperatures less than 600°C and the second, bigger mass loss occurs at temperatures greater than 800°C. The first mass loss is significant for lower milling periods and is the highest for cryogenic attritor milling. As the milling period is increased, the mass loss decreases and eventually there is no mass loss. This trend is observed over all conditions and milling equipment.

The gaseous products emanating from the mass in temperatures below 600°C show presence of CF<sub>2</sub>, CF<sub>3</sub>, C<sub>2</sub>F<sub>3</sub> and C<sub>2</sub>F<sub>4</sub> when analyzed under the mass spectrometer, run in line with the TG equipment. The second mass loss in materials with no initial mass loss was expected to be 10% or less which would be indicative of losing PTFE from the system. But the loss is over 15% as can be seen for 6-hour cryomilled sample in Figure 3.5. The gaseous products exuding at temperatures greater than 800°C could not be

analyzed in the spectrometer. This could probably be caused by the difficulty in analyzing gaseous products that aren't stable or products that need high temperatures to exist in gas phase which the entry arm of the mass spectrometer doesn't guarantee.

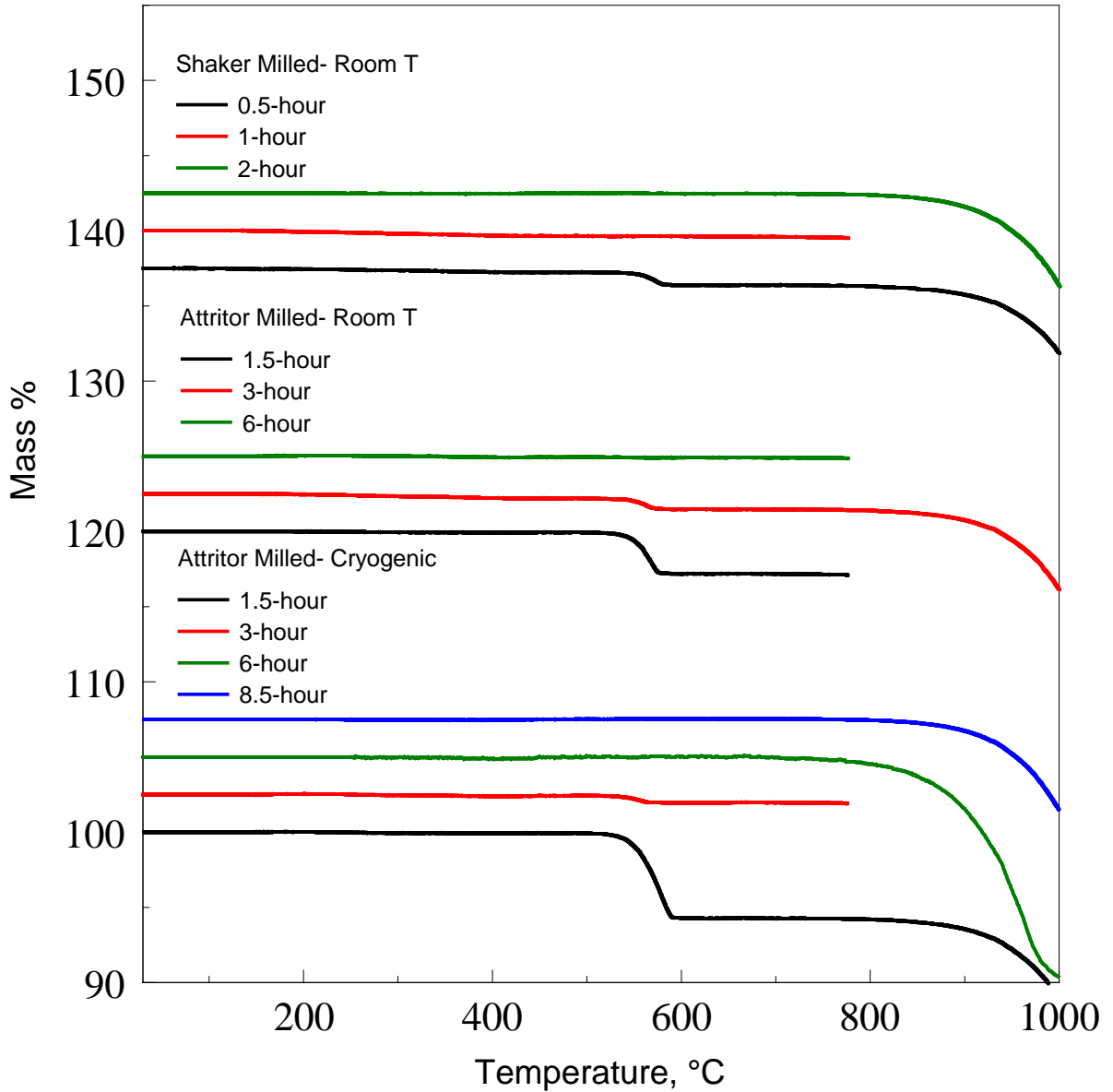


**Figure 3.5** TG plots of all Al-PTFE (90-10 wt. %) milled material in anaerobic environment (100ml/min argon) in a temperature range of 30°C-1000°C with a heating rate of 20K/min.

The corresponding DTA plot for the anaerobic study can be viewed in Figure 3.6.

The common feature for all the materials prepared is that they exhibit two exotherms in the region 350°C -600°C and the aluminum melting event observable as an endotherm, at 660°C. In general for all equipment and conditions, the second exotherm diminishes and moves closer to the first exotherm with milling time.

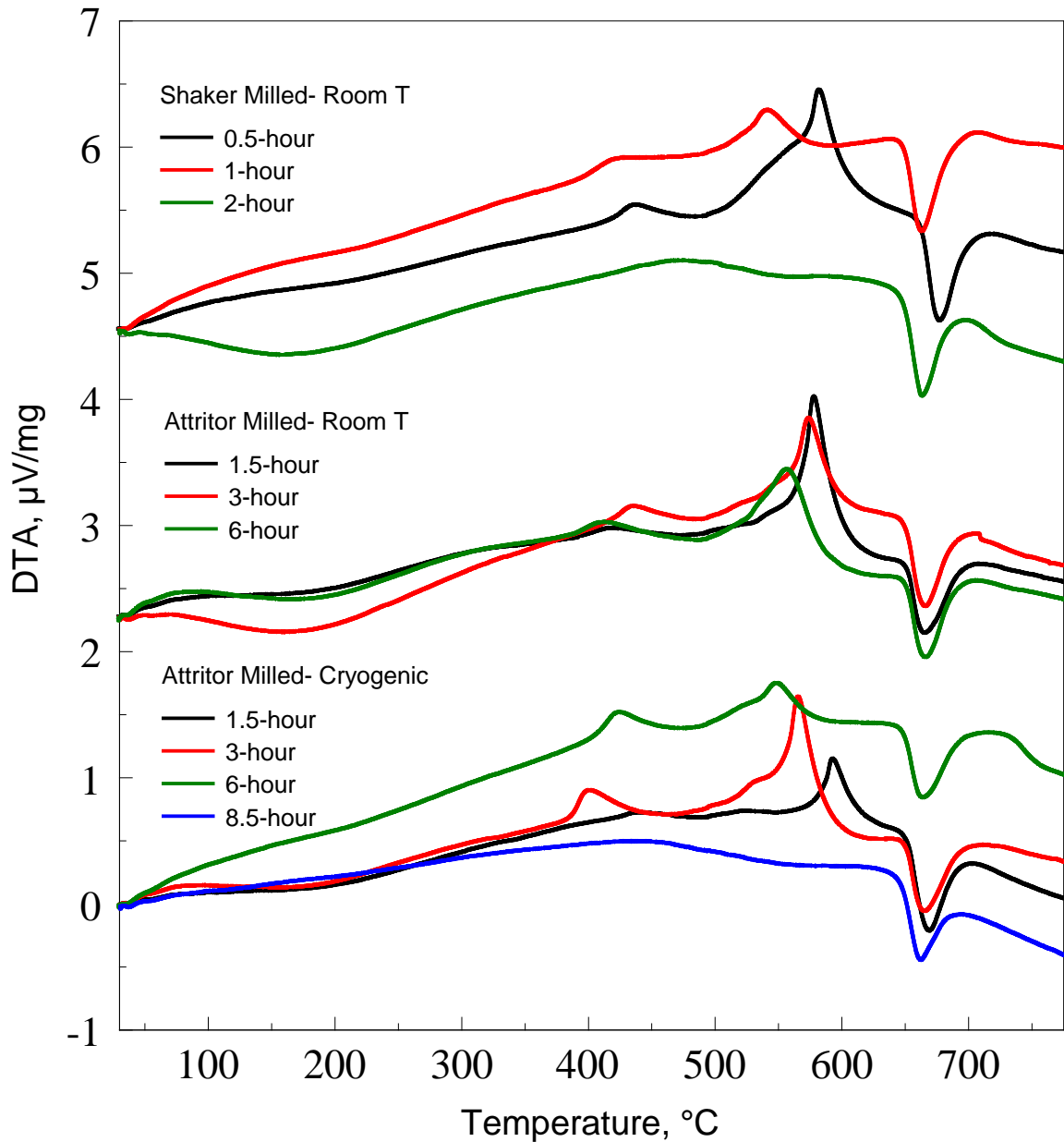


**Figure 3.6** DTA plots of all Al-PTFE (90-10 wt. %) milled material in anaerobic environment (100ml/min of argon) in a temperature range of 30 $^{\circ}\text{C}$ -775 $^{\circ}\text{C}$  with a heating rate of 20K/min.

The trends across shaker milled and cryogenic attritor milled samples seem comparable while the room temperature attritor milling seems to follow a slightly different trend; the shift and loss in prominence of the second exothermic peak with milling, is not as pronounced. For longer milling periods, the two exotherms come together as an indistinctive wide exothermic event. On closer observation we see a small exothermic event between the two exotherms which can be seen for 1.5-hour cryogenic attritor milled sample. As the second exotherm shifts to lower temperatures, towards the first exotherm, this intermediate exothermic event is overlapped with the second exotherm and thus gaining strength. This interim exothermic event can be seen as a shoulder to the second exotherm for most of the samples. The second exotherm coincides with the initial mass loss observed in temperatures below 600°C, as seen in Figure 3.5 and loses prominence just as the mass loss decreases with milling.

From the thermal analysis in anaerobic atmosphere of the 6-hour cryomilled sample, kinetic studies were conducted. Using different heating rates and the peak positions of the two exotherms seen in Figure 3.7 and Figure 3.6, we calculate the activation energy of the two reactions using Kissinger's method which is described in detail elsewhere (Kissinger, 1957). The activation energies for the first and second exothermic reactions are close to 145.8 and 266.4 kJ/mol, respectively. The Kissinger plots are which are shown in Figure 3.8. Further, the activation energy of the second exotherm at 266.4 kJ/mol is in good agreement with the activation energy of aluminum oxide and PTFE system (265kJ/mol) as calculated by Hobosyan et al, 2014. In the same work, Hobosyan et al also match this to the decomposition energy of PTFE.



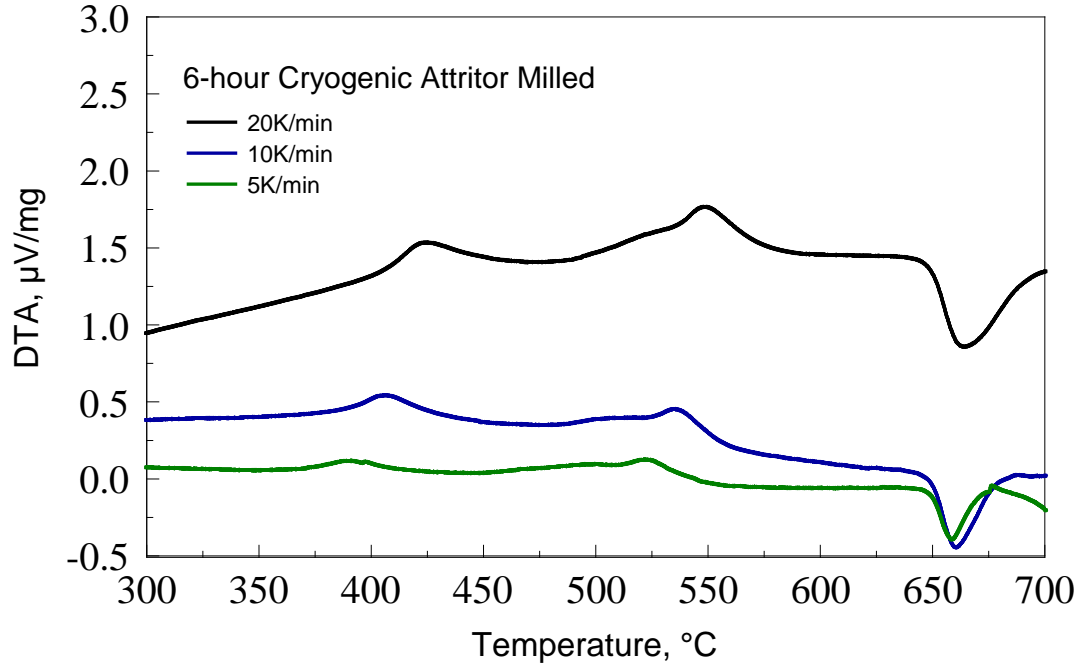


**Figure 3.7** DTA plots in anaerobic environment (100ml/min of argon) in a temperature range of 250°C-700°C with various heating rates (5K/min, 10K/min, 20K/min) of CM-6; 6-hour cryogenic attritor milled Al-PTFE (90-10 wt. %) milled material.

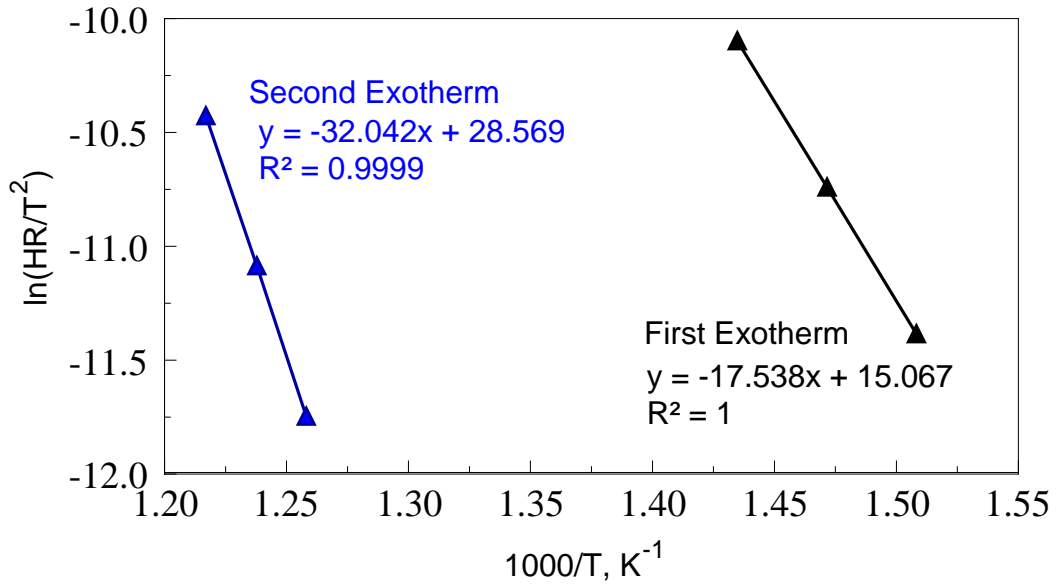


**Figure 3.8** Kissinger plots for the two minor exotherms observed in the temperature range of 350°C-600°C with various heating rates (5K/min, 10K/min, 20K/min) of CM-6; 6-hour cryogenic attritor milled Al-PTFE (90-10 wt. %) milled material.

Thermal analysis in an oxidizing environment has been conducted for all the milled materials at 5 K/min; the results are presented in Figure 3.9. All the samples exhibit qualitatively similar curves with initial weight loss at lower temperatures (400 – 520 °C), an oxidation step after that between 600 and 750 °C and further oxidation at temperature.

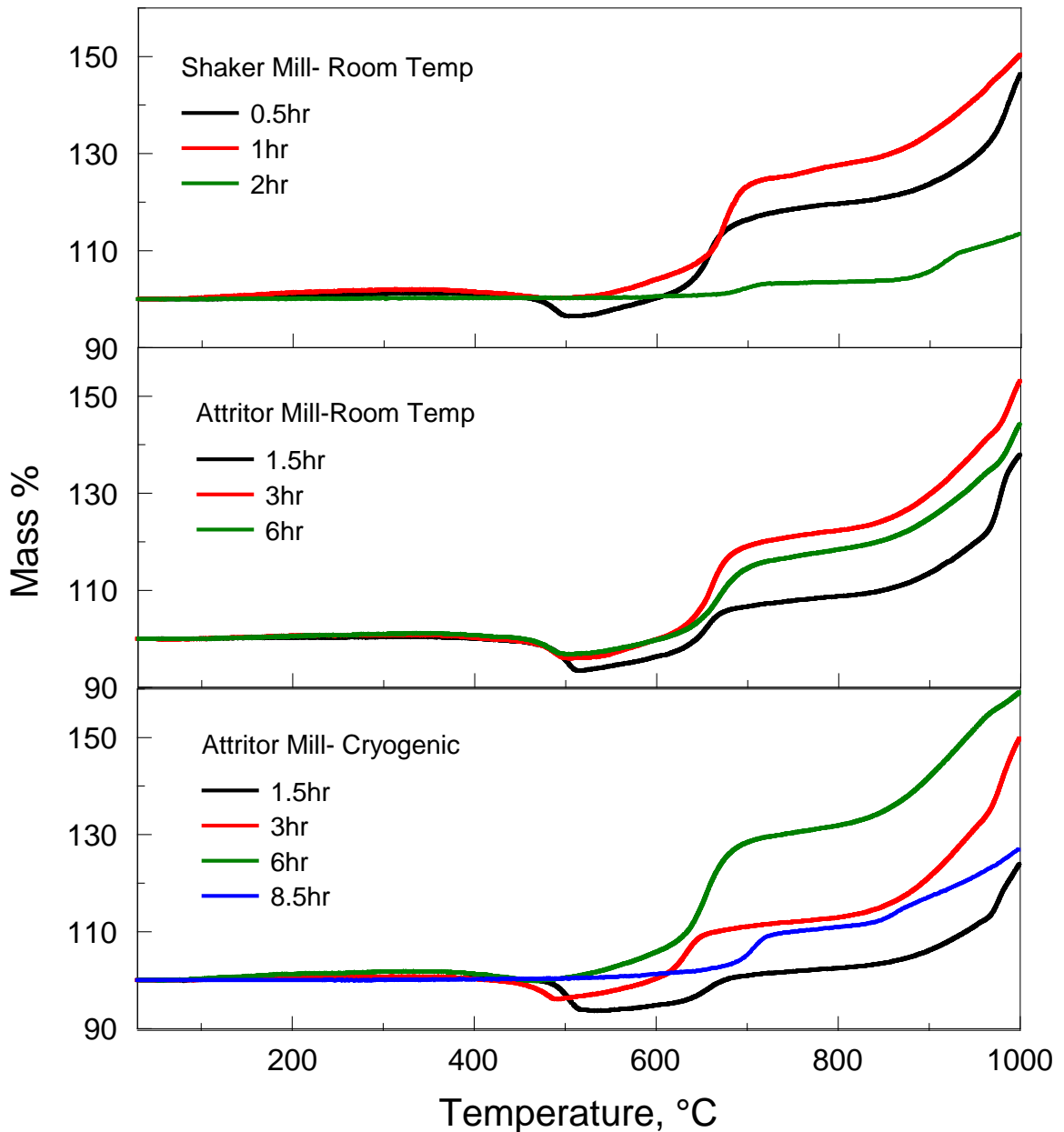


**Figure 3.9** TG plots of all Al-PTFE (90-10 wt. %) milled material in aerobic environment (100ml/min of oxygen and argon; 50-50 v/v) in a temperature range of 30°C-1000°C with a heating rate of 5K/min.

The mass loss observed between 400°C-500°C is in the vicinity of exothermic events observable in their corresponding DTA plots in Figure 3.10. In general this mass loss decreases as milling time increases until there is no mass loss observable. The use of Mass Spectrometry in line with TG measurements show that CO<sub>2</sub> is the primary product with CF<sub>3</sub>, C<sub>2</sub>F<sub>3</sub> and C<sub>2</sub>F<sub>4</sub> being the other products.

For the shaker-milled samples, the mass gain shifts to a lower temperature when the milling time is increased from 0.5-hour to 1-hour. However, the mass gain occurs at a higher temperature, when the milling time is increased further, to 2-hour. A second oxidation step is observed at higher temperatures, e.g. around 900 °C.

For the samples prepared in the attritor mill at room temperature, the decrease in initial mass loss with milling time is not very substantial. The change in the mass loss is significant between the samples milled for 1.5 and 3-hour. However, the mass loss is nearly the same for the samples milled 3 and 6-hour. The first oxidation step occurs at a lower temperature for the sample milled for 3-hour compared to that milled for 1.5-hour. For the sample milled for 6-hour, the onset and mass gain of the first oxidation step is nearly identical to that for the 3-hour milled sample.

For the cryomilled samples, the initial mass loss is consistently diminishing with an increased milling time. The first oxidation step shifts to lower temperatures and becomes increasingly stronger, as the milling times increase from 1.5 to 6-hour. However, it occurs at a substantially higher temperature and becomes weaker for the longest milling time of 8.5-hour. At 130% the CM-6 (6-hour cryogenic attritor milled sample) mass gain for the first oxidation step, is the highest as compared to all other samples.

The corresponding DTA plots for the oxidative analysis show all samples with two major exothermic events (at around 600°C and 1000°C) and two more minor exothermic events (at around 400°C and 500°C respectively). These two minor exothermic events are visible as a small peaks for lower milling periods, gradually become less prominent. The minor exothermic peaks observed in the oxidizing environment occur at similar temperatures as those observed in the experiments performed in argon, Figure. 3.6. The second minor exotherm coincides with the weight loss observed in the respective TG curves. The first major exothermic peak coincides with the weight gain corresponding to the first oxidation step observed in TG curves; the second major exotherm at higher temperatures correlates with the second oxidation step.

The curves also shift to higher levels as milling time progresses till a milling time beyond which they return. The second exothermic peak occurring in the range 600°C to 750°C coincide with an endothermic peak at 660°C. This exothermic peak occurs during the weight gain step observed in Figure 3.8. The room temperature shaker mill sample, SM-1 (1-hour milled) and cryogenically attritor milled sample, CM-6 (6-hour milled) samples show the highest exothermic peaks at the weight gain step. The peak for the cryogenically milled sample however begins at a lower temperature.

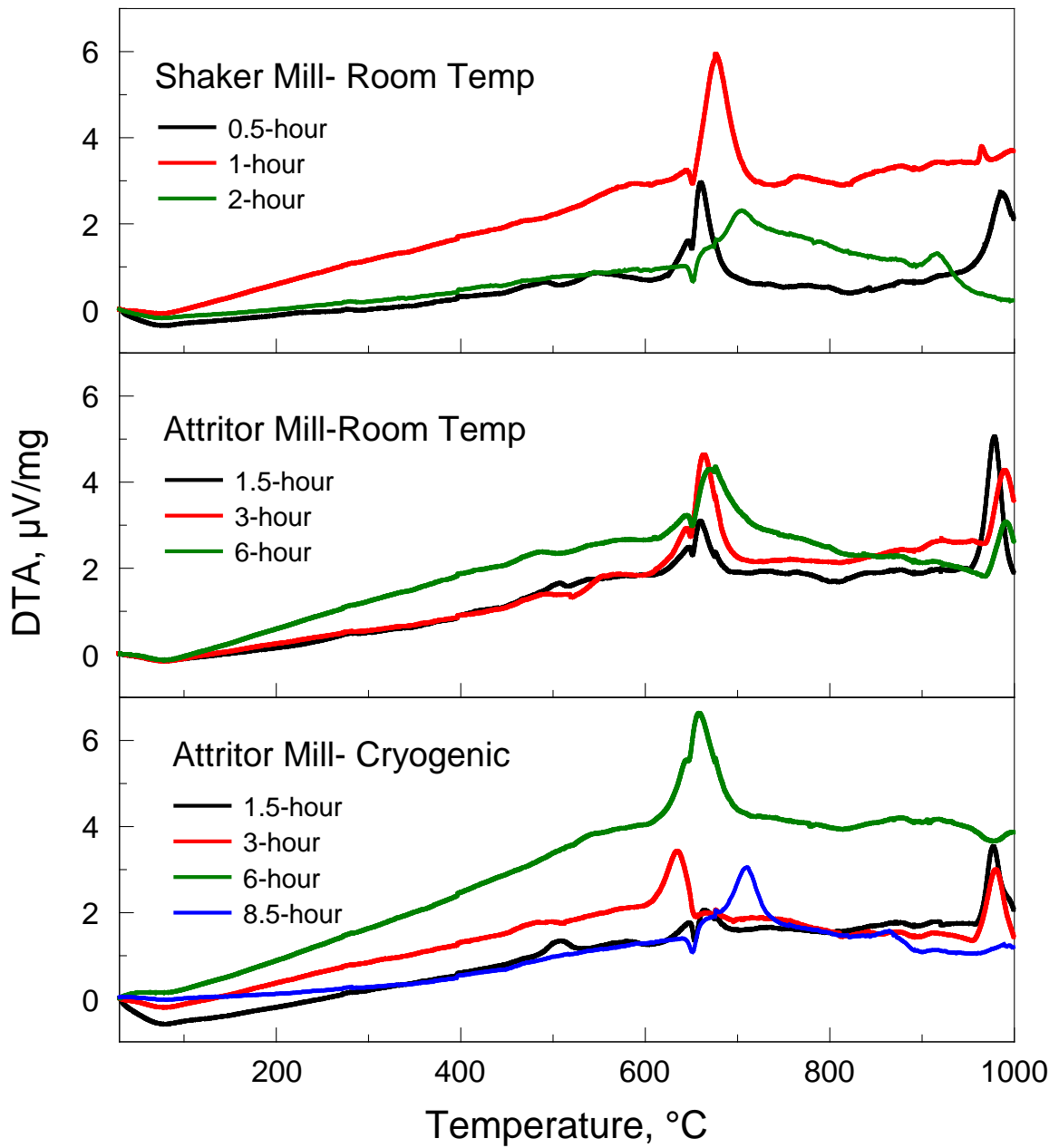


**Figure 3.10** DTA plots of all Al-PTFE (90-10 wt. %) milled material in aerobic environment (100ml/min of oxygen and argon; 50-50 v/v) in a temperature range of 30°C-1000°C with a heating rate of 5K/min.

### 3.1.3 XRD Analysis

The preliminary study of Al-PTFE system with Al dominated matrix, consisted of analysis of Al-PTFE milled sample of composition (95-5 wt. %). The material was prepared by shaker milling with a milling time of two hours. It can be seen from the Figure 3.10, that the fresh sample consists of just aluminum peaks and no crystalline PTFE. At 700°C, we see presence of  $\text{AlF}_3$  and also the beginning of Aluminum Carbides ( $\text{Al}_4\text{C}_3$ ) formation. At even higher temperatures we observe that the Aluminum trifluoride is not observable anymore. This is understandable in the point of observation, 1200°C, is close to the sublimation temperature of  $\text{AlF}_3$  and its vapor pressure is substantial. We also see stronger peaks of carbides and carboxides of Aluminum at these high temperatures.

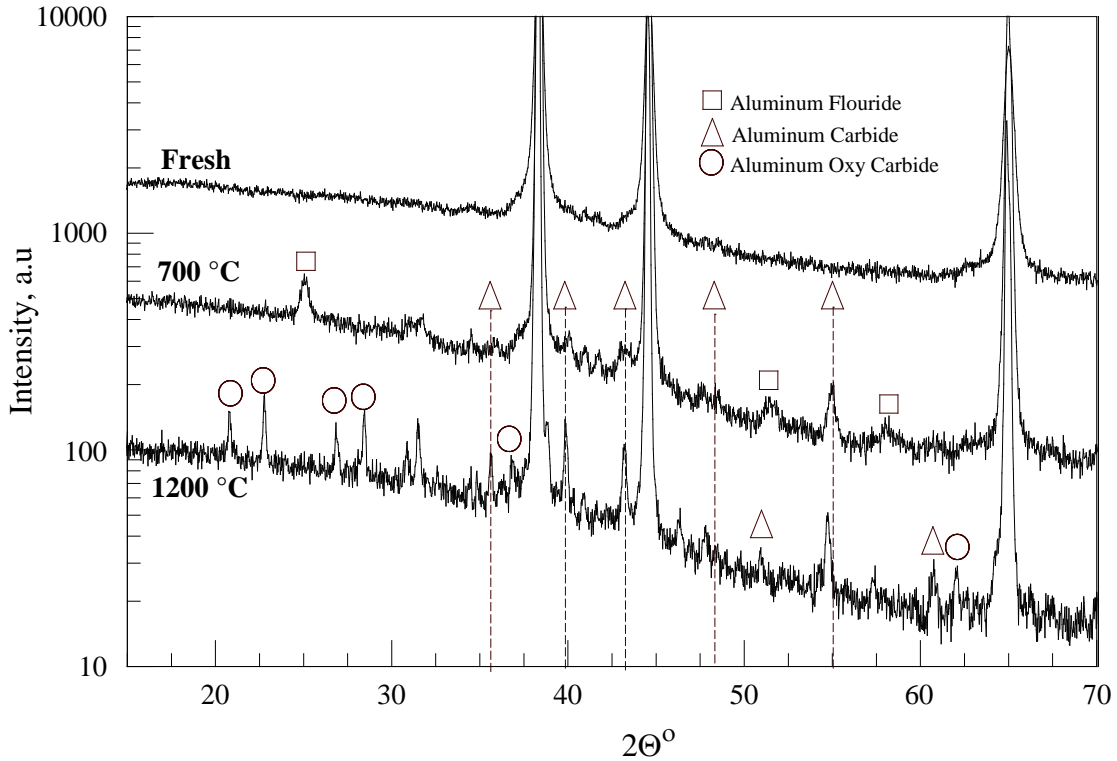


**Figure 3.11** Preliminary Study with XRD patterns of Al-PTFE (95-5 wt. %) shaker milled material and quenched samples in anaerobic environment (100ml/min of argon).

Figure 3.11 shows the XRD analysis of freshly made samples for comparable milling periods (The comparison between shaker and attritor mill is as established by (Santhanam, 2012)). All strong unmarked peaks are produced by aluminum. The figure shows that PTFE could be absent or present in a different form for the 2-hour room temperature milling in the shaker mill. The PTFE peak is strongest for 6-hour room temperature, attritor milled sample and is also weakly visible in its cryogenic counterpart.

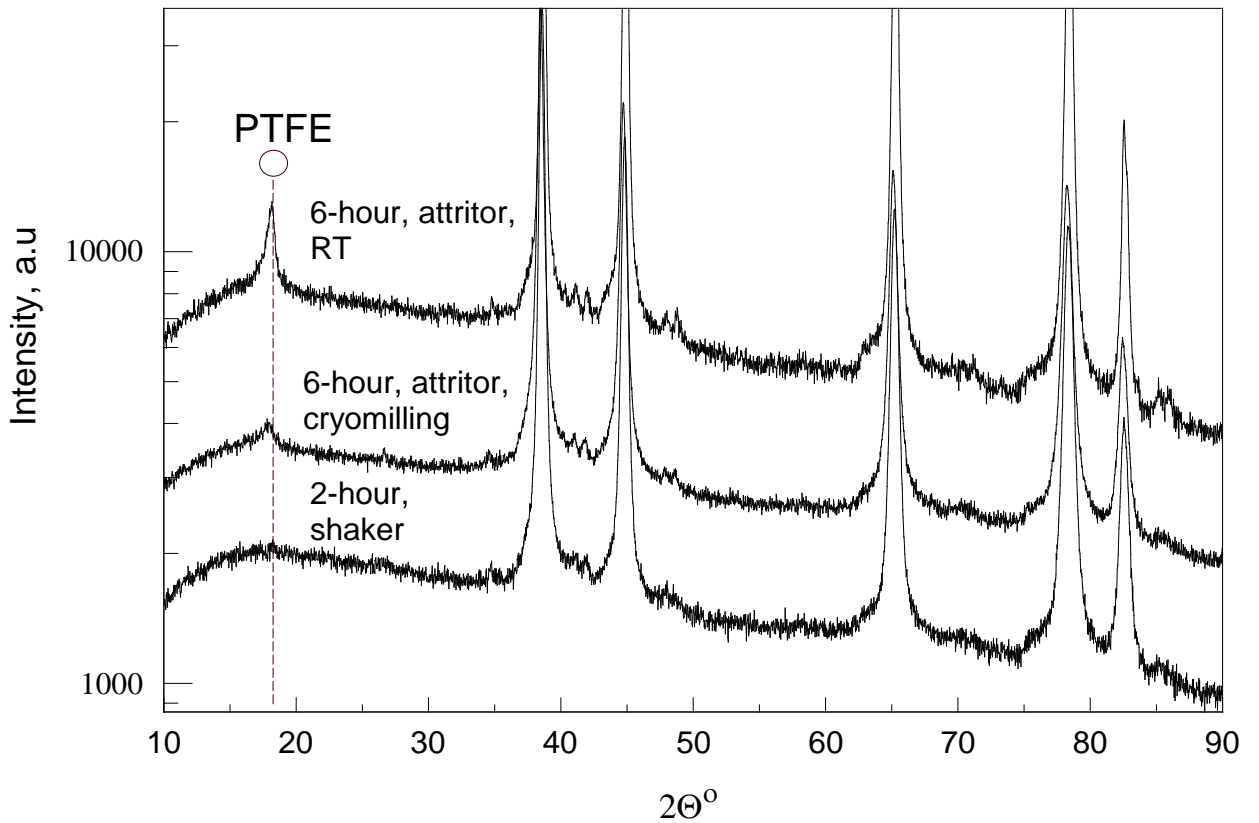


**Figure 3.12** XRD patterns of freshly prepared of Al-PTFE (90-10 wt. %) composition for comparable samples prepared by milling in shaker mill for 2-hour and attritor mill at room temperatures and cryogenic temperatures for 6-hour milling periods.

To study the effect of milling duration in cryogenic attritor milling, the samples from different milling periods have also been analyzed. Figure 3.12 shows the XRD

patterns of 1.5-hour, 6-hour and 8.5-hour cryomilled samples. As the milling duration increases we see a clear broadening and decrease in intensity of aluminum peaks. This is a clear indication of size reduction with longer milling. The second notable change is that the PTFE peak gradually loses prominence and disappears with milling time. This could possibly mean the consumption in PTFE during milling or a change in morphology.

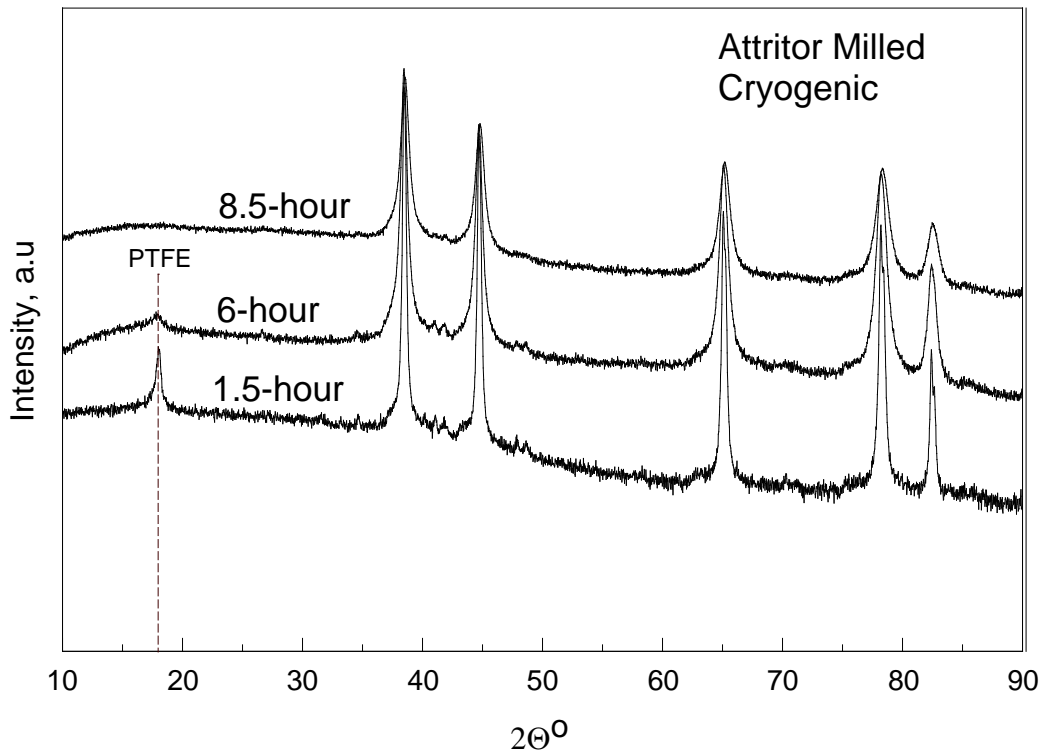


**Figure 3.13** XRD patterns of Al-PTFE (90-10 wt. %) attritor mill samples prepared at cryogenic temperatures for various milling periods (1.5-hour, 6-hour, 8.5-hour).

To study the change in samples after their first weight loss in oxidative thermal studies, materials were quenched, recovered and studied by XRD. Cryomilled samples of prepared during 1.5 and 6-hour were analyzed. Figure 3.13 show the XRD patterns of freshly prepared 6-hour and 1.5-hour cryomilled samples and their respective samples recovered after their first weight loss. Fresh samples exhibit PTFE peaks at 18 degrees



while samples collected after the first weight loss do not show this peak. This could possibly mean that the initial weight loss observed in the oxidative thermal analysis could be the loss of PTFE which was not incorporated into the milled powder on a microscopic scale.

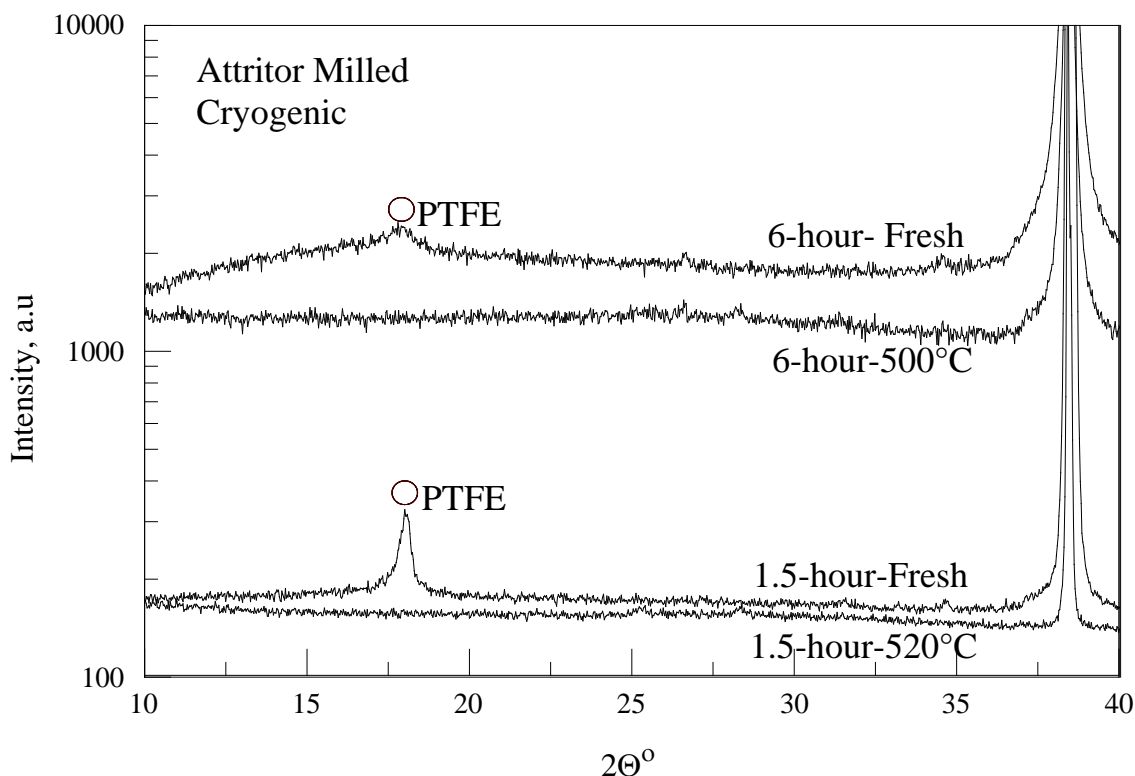


**Figure 3.14** XRD patterns of Al-PTFE (90-10 wt. %) attritor mill samples prepared at cryogenic temperatures for various milling periods (1.5-hour and 6-hour) and their respective samples after their first weight loss in oxidative thermal analysis.

To carry forward the same line of thought over the entire range of thermal analysis for an anaerobic environment, a 1-hour Shaker Milled sample was quenched at various significant temperatures and analyzed in XRD. Figure 3.14 shows the XRD patterns of a freshly prepared sample and those collected after the first exotherm ( $\sim 480^\circ\text{C}$ ), the second exotherm ( $\sim 600^\circ\text{C}$ ), at the start of mass loss observed at a higher temperature ( $\sim 775^\circ\text{C}$ ) and towards the end of mass loss ( $\sim 1000^\circ\text{C}$ ). We see that by  $480^\circ\text{C}$  we lose the small PTFE peak

and see small aluminum carbide peaks beginning to show. This corresponding with the very small mass loss in the same temperature range.

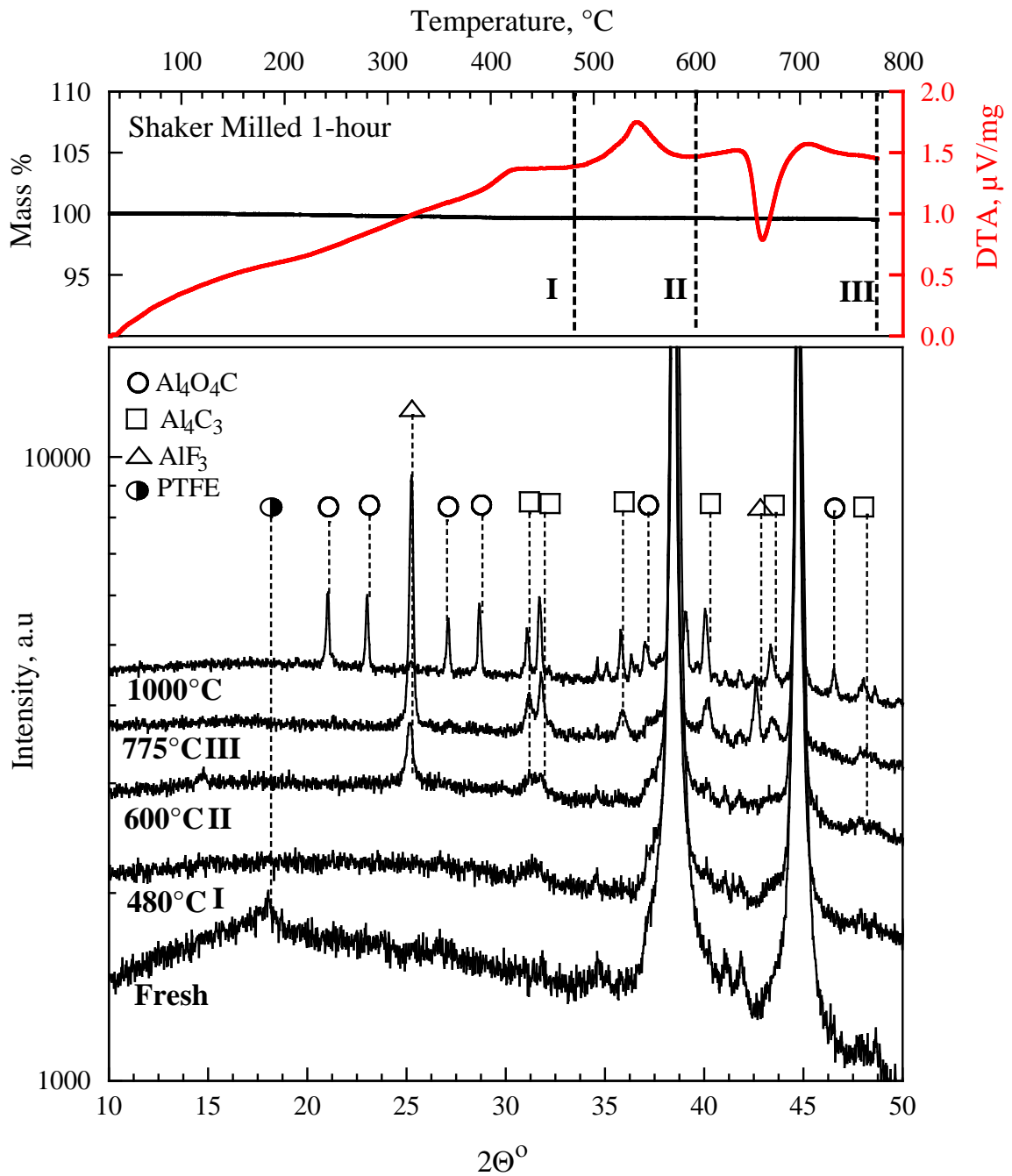


**Figure 3.15** XRD patterns of Al-PTFE (90-10 wt. %) shaker milled samples collected at various temperatures (30°C, 480°C, 600°C, 775°C and 1000°C) and corresponding TG/DTA significance of collected samples.

At 600°C we see  $\text{AlF}_3$  peaks and the aluminum carbide starting to gain prominence. We may say that the second exothermic event results in the formation of the fluoride. As we go across the aluminum melting event and towards the start of the mass loss at 775°C, we observe strong  $\text{AlF}_3$  peaks and carbide peaks. At higher temperatures after the mass loss at 1000°C, we see no  $\text{AlF}_3$  peaks. We see formation of carboxides and stronger carbide peaks as observed in the preliminary study with Al-PTFE (95-5 wt. %). Also we see a clear sharpening of aluminum peaks due to the crystallographic changes it experiences. The two unexplained small peaks between the aluminum peaks at 38 and 44 could be aluminum oxide as they are present even in the fresh sample and slowly lose prominence as fluorides and carboxides of aluminum are formed.

#### **3.1.4 ESD Experiment**

The ESD experiment was conducted for all the milled material. All the room temperature milled material in both the attritor mill and the shaker mill did not ignite despite being flaky and being sparked with high energy. The cryogenic attritor milled samples however ignite when high energy was supplied (12 kV and 10000 pF capacitance). The lower cryomilled samples are harder to ignite and do not very produce reproducible results. The higher milling duration samples (CM-6, CM-8.5) however show results that are reproducible. Figure 3.15 shows the pressure generated in the ESD chamber as a function of time for the two longer milling runs; 6-hour and 8.5-hour.

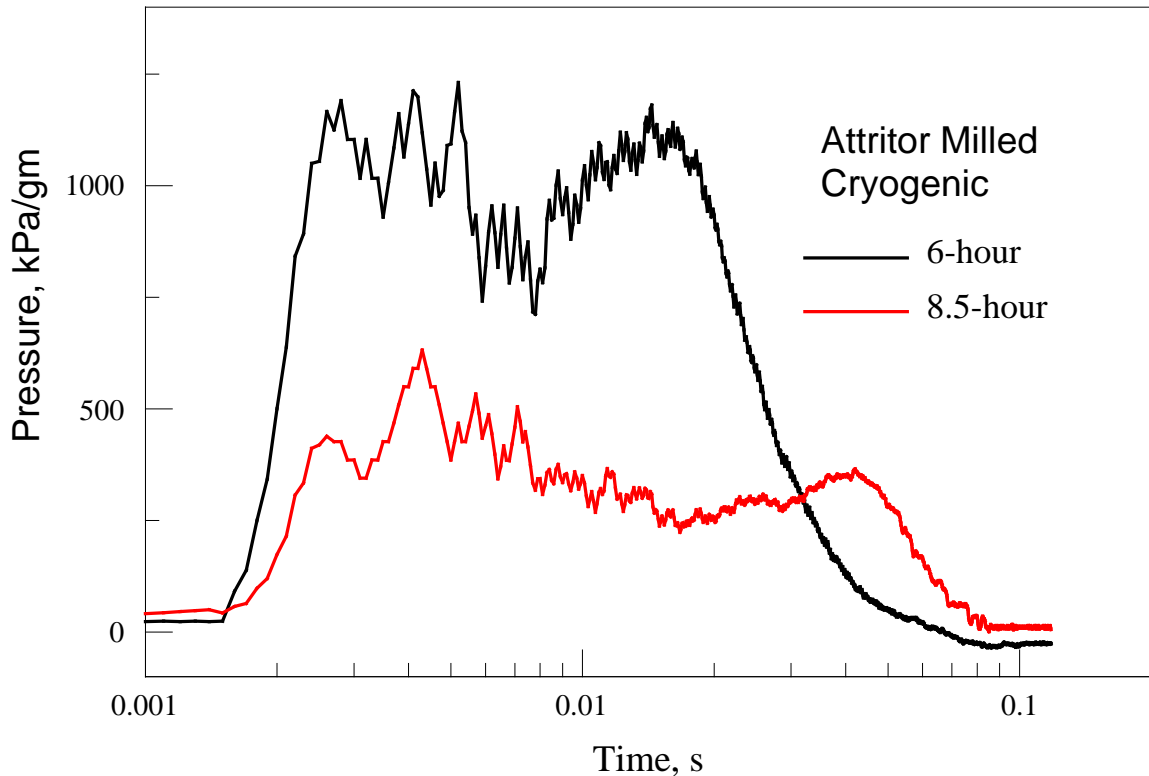


**Figure 3.16** The Pressure plot generated in ESD (12kV, 10000pf capacitance) for 6-hour and 8.5-hour attritor milled at cryogenic temperature samples.

The pressure plots show two peaks for both the samples, where the first stronger peak is a very fast event. The second smaller pressure peak occurs at a later time and tails off. Due to the time duration difference in the two events the resolution of only one could be captured (in the Figure 3.12 the second peak is the primary focus) rendering the first speak jagged and with poorer resolution. The 6-hour cryomilled sample shows a stronger peak and is faster than the longer milled 8.5-hour sample. The peaks for the longer milled sample are broader (longer events) and less than half as intense (lower pressure rises).

The light emission captured by the PMT during ESD ignition measured as a function of time is represented in Figure 3.16. The emissions for the longer milled sample shows two peaks at lower intensities over a long time scale. The emission peaks for the shorter milling of 6hour come very close to give a single sharper peak of higher intensity.

The event starts sooner for the 8.5-hour longer milled sample and last longer even but the intensity of the event is much smaller.

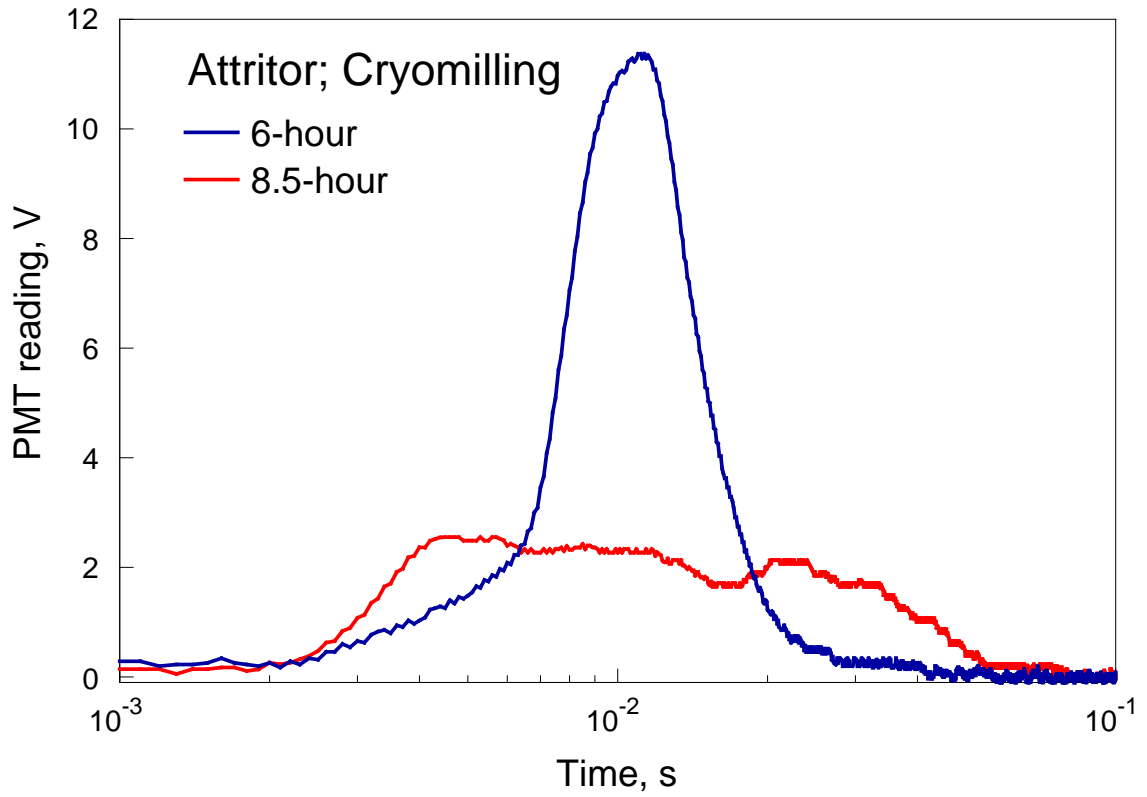


**Figure 3.17** The Light emission plot during ESD (12kV, 10000pf capacitance) for 6-hour and 8.5-hour attritor milled at cryogenic temperature samples.

## **3.2 Discussions**

### **3.2.1 Best Performing Material**

The 6-hour cryomilled sample (CM-6) shows the greatest exothermic reaction of all the materials in an oxidative environment. It also gains the most weight during that oxidation process. It may be said that whatever little PTFE remains that is not properly dispersed escapes the system at lower temperatures; an explanation for initial weight loss. Despite its uniform distribution of PTFE in its bulk, the XRD analysis shows a very weak PTFE signal. This weak signal is gone after its first weight loss, a similar very small weight loss is observant in the TG measurements in oxidative environment. From this it may be concluded that 6-hour milling is close to the optimum period for the cryogenic milling of Al-PTFE (90-10 wt. %) in the attritor at cryogenic temperatures. The CM-6 sample also shows ignition in the ESD unlike room temperature milled material and also generates the highest pressure during the process. The next best material is 1-hour shaker milled sample (SM-1) which has qualitatively comparable behavior in thermal analysis.

### **3.2.2 Comparison with Other Al-PTFE Preparations**

The anaerobic thermal analysis of 6-hour cryomilled Al-PTFE (90-10 wt. %) sample exhibits a behavior markedly different than other milled Al-PTFE composites. The Figure 3.17 compares the composites prepared by Sippel et al. Al-PTFE (70-30 wt. %) with the 6-hour cryomilled sample. The 6-hour cryomilled sample (CM-6) does not lose weight till a high temperature of over 850°C when heated at the rate of 20K/min. While the 1 hour, room temperature, shaker milled sample of composition Al-PTFE (70-30 wt. %) as shown by (Sippel et al., 2013a) begins to lose weight even before PTFE weight loss temperatures. The low energy composite of the same composition prepared by (Sippel et

al., 2013a) and the nano powder aluminum and nano size PTFE blend prepared by (Osborne & Pantoya, 2007) lose weight at a temperature comparable to that PTFE. From this we may see that cryomilling has ensured that we retain the PTFE in the material in some form till a higher temperature before it is lost.

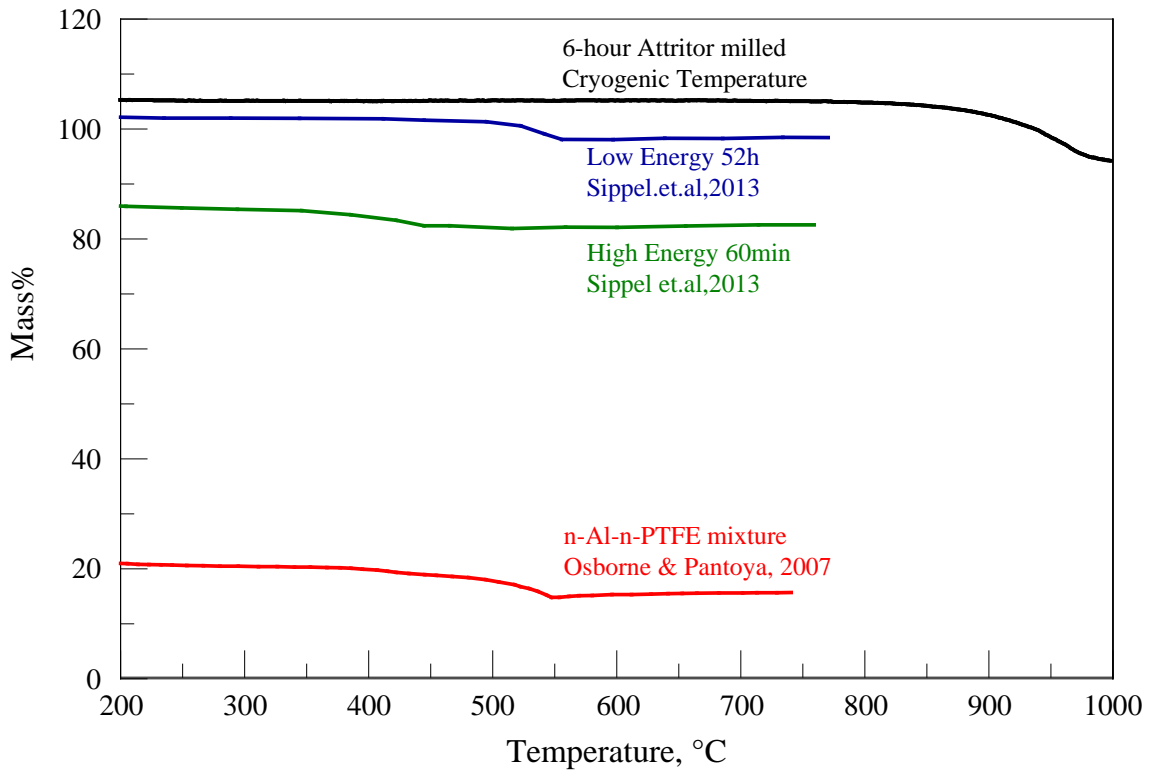


**Figure 3.18** Comparison of TG plots in anaerobic environment (20K/min, argon atmosphere) in a temperature range of 100°C-1000°C among various Al-PTFE samples; 6-hour cryogenic attritor milled Al-PTFE (90-10 wt. %) and Al-PTFE (70-30 wt. %) composition milled materials and mixtures by (Sippel et al., 2013a)

The energy changes occurring in the different room temperature milled Al-PTFE (70-30 wt. %) samples prepared by (Sippel et al., 2013a) and the 6-hour cryomilled Al-PTFE (90-10 wt. %) sample may be compared by putting together the DSC and DTA plots respectively as shown in Figure 3.18. The plot compares the temperatures at which changes occur in a quantitative fashion between the aforementioned materials. The two

exothermic peaks are in the range of 380°C- 480°C and 480-580°C. An endotherm is observed in all four at 660°C, which is the melting point of aluminum. The exothermic reactions occur at a lower temperatures for the 6-hour cryomilled Al-PTFE (90-10 wt. %) sample as compared to the room temperature milled material prepared by Sippel et al.

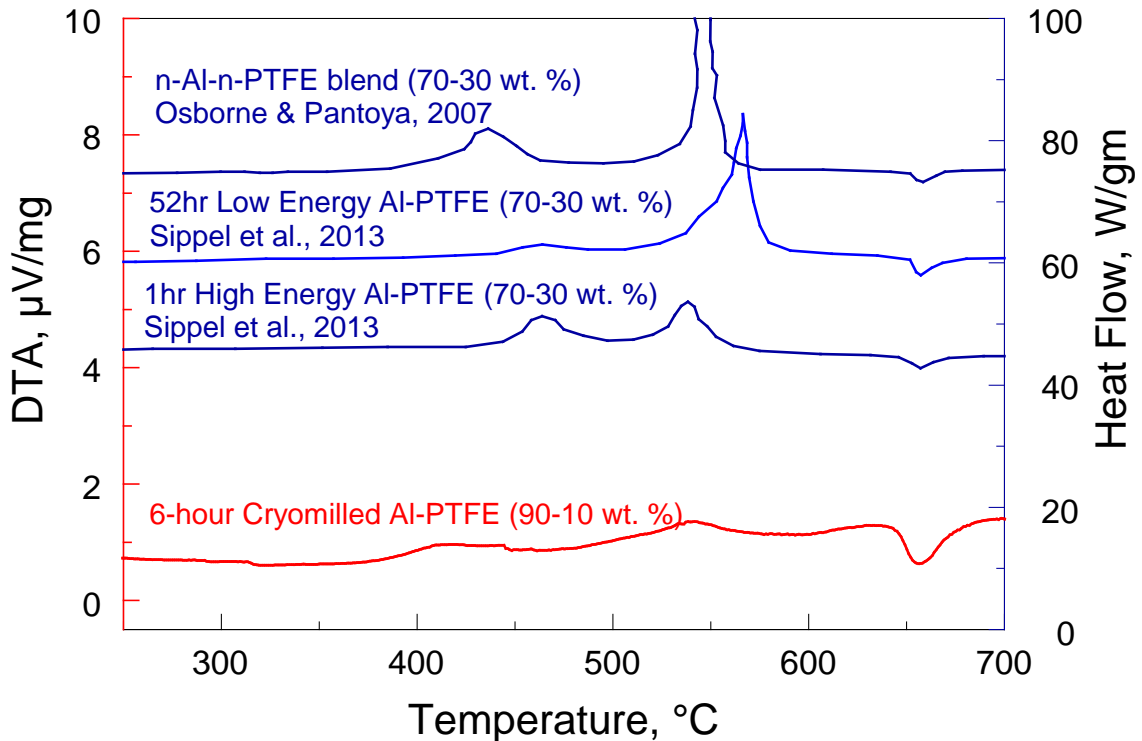


**Figure 3.19** Comparison in anaerobic environment (20K/min, argon atmosphere) in a temperature range of 250°C-700°C among various Al-PTFE samples; DTA plot of 6-hour cryogenic attritor milled Al-PTFE (90-10 wt. %) and DSC plots of Al-PTFE (70-30 wt. %) composition milled materials and mixtures by (Sippel et al., 2013a) and n-Al-n-PTFE (70-30 wt. %) blend by (Osborne & Pantoya, 2007).

The two exothermic peaks are of comparable sizes for both the room temperature high energy shaker milled Al-PTFE (70-30 wt. %) sample and the 6-hour cryomilled Al-PTFE (90-10 wt. %) sample but occur at slightly lower temperatures for the cryomilled sample. A similar pattern of energy changes is also observed in nano-aluminum and nano- PTFE blend (Osborne & Pantoya, 2007). The exothermic events occur at almost



the same temperatures for the 6-hour cryomilled Al-PTFE (90-10 wt. %) sample and Osborne & Pantoya's nano-Al and nano-PTFE blend (70-30 wt. %). These two minor exothermic peaks occurring near 400°C and 500°C become even less prominent as milling duration increases as seen in earlier in Figure 3.6. These minor exothermic peaks correspond with two stage ignition of nano-sized blend of Al-PTFE (70-30 wt. %) as proposed by (Osborne & Pantoya, 2007). Despite the minor exothermic peaks losing prominence over milling time, the subsequent exothermic peak from first oxidation becomes huge.

## CHAPTER 4

### CONCLUSIONS

This work addressed composite Al-PTFE materials with high, 90 wt% concentration of aluminum. Such materials are attractive as advanced fuels, because of their high reaction enthalpy approaching that of the pure aluminum; at the same time, their reaction dynamics is expected to be changed markedly because of the added fluorinated compound. Flake-like powders are produced by ball-milling aluminum and PTFE; the powders become more equiaxial at longer milling time when the milling is performed at the cryogenic temperature. Cryomilling produces a composite aluminum-PTFE material with the polymer distributed more uniformly than in the similarly prepared samples milled at room temperature. When PTFE is distributed homogeneously, it stops producing the characteristic XRD pattern that can be assigned to the PTFE structure; it also does not volatilize at its normal evaporation temperature. The fluorinated compound is retained in the composite material when it is heated at least 100 °C above the normal PTFE volatilization point; it is volatilized at that time when the material is heated in the inert environment. A part of PTFE captured in the voids and crevices of the prepared samples, volatilizes as bulk PTFE, generating respective weight loss observed in the TG traces.

Two low-temperature and relatively minor exothermic events around 400 and 500 °C were observed upon heating of the prepared composite materials in both inert and oxidizing environments. The first event is not associated with any weight change and occurs at the temperatures similar to those of the reported reaction of hydroxyl groups

attached to surface of alumina interacting with PTFE and leading to the formation of  $\beta$ - $\text{AlF}_3$  (Sarbak.Z, 1997). The second event occurs in vicinity of the reported polymorphic phase change between  $\beta$ - and  $\alpha$ - $\text{AlF}_3$ , when  $\beta$ - $\text{AlF}_3$  becomes metastable (Sarbak.Z, 1997). This event coincides with the volatilization of a part of PTFE when heating occurs in an oxidizing environment. This could be explained by weakening Al-F bonds caused by the phase change, and oxidation of aluminum exposed to the oxidizing environment. As a result, both weight gain and weight loss can occur, caused respectively by evaporation of fluorine and absorption of oxygen. Experimentally, it appears that weight loss effect is dominant. However, no detectable weight loss is observed in the inert environment, suggesting no removal of fluorine in the absence of oxygen. The activation energies of the exothermic reactions at 405.4°C and 540°C are 145.8 and 266.4 kJ/mol respectively. Both events become weaker for the samples prepared using longer milling times. These events are qualitatively similar to pre-ignition reactions identified for aluminum-PTFE composites in earlier work. The relative strength of these events correlates qualitatively with the flammability of powder samples ignited when placed on a burning paper. However, the strength of the respective exothermic peaks does not correlate with the ability of the prepared materials to be ignited by electrostatic discharge. Therefore, it is suggested that qualitatively different ignition mechanisms are responsible for initiation of these materials heated at varied heating rates.

Two major exothermic events accompanied with weight increase are observed when the prepared composite powders are heated in an oxidizing environment. In particular, the first oxidation step occurring for some materials at the temperatures lower than the aluminum melting point, is expected to be important in controlling ignition of

such materials. It was observed that for the material cryomilled for 6 hours, the first oxidation step occurs at the lowest temperatures and is accompanied with the greatest mass gain and heat release among all other prepared materials. Note that because both longer and shorter milling times were used, the 6-hour cryo-milled sample appears to be optimized for the applications in energetic formulations. This material is also observed to produce strongest optical emission and pressure pulses when ignited by electrostatic discharge. None of the materials milled at room temperature could be ignited at comparable ESD energies.

## REFERENCES

- Belov, B. V. (2004). REAL for windows. Moscow.
- Cudzilo, S.; Trzcinski, W.A. (2001). Calorimetric Studies of Metal/Polytetrafluoroethylene Pyrolants. *Polish Journal of Applied Chemistry*, XLIV(1-2), 25-32.
- Dolgoborodov, A. Y.; Makhov, M.N; Kolbanev,I.V; Streletskii,A.N; Fortov,V.E. (2005). Detonation in Aluminum-Teflon Mixture. *JETP Letters*, 81(7).
- Hobosyan, M. A., Kirakosyan, K. G., Kharatyan, S. L., & Martirosyan, K. S. (2014). PTFE–Al<sub>2</sub>O<sub>3</sub> reactive interaction at high heating rates. *Journal of Thermal Analysis and Calorimetry*, 119(1), 245-251. doi: 10.1007/s10973-014-4080-0
- Kissinger, H. E. (1957). Reaction Kinetics in Differential Thermal Analysis *National Bureau of Standards*.
- Koch, E.-C., Hahma, A., Weiser, V., Roth, E., & Knapp, S. (2012). Metal-Fluorocarbon Pyrolants. XIII: High Performance Infrared Decoy Flare Compositions Based on MgB<sub>2</sub> and Mg<sub>2</sub>Si and Polytetrafluoroethylene/Viton®. *Propellants, Explosives, Pyrotechnics*, 37(4), 432-438. doi: 10.1002/prop.201200044
- Kubota, N., and Serizawa,C. (1987). Combustion of Magnesium/Polytertrafluoroethylene. *Journal of Propulsion*, 3(4), 303-307.
- Lips, H. R. (1977). Experimental Investigation on Hybrid Rocket Engines Using Highly Aluminized Fuels. *Journal of Spacecraft*, 14(9).
- Losada, M. C., S. (2009). Theoretical Study of Elementary Steps in Reactions between Aluminum and Teflon Fragments under Combustive Environments. *Journal of Physical Chemistry*, 113, 5933-5941.
- Maggi, F., Dossi, S., Paravan, C., DeLuca, L. T., & Liljedahl, M. (2015). Activated aluminum powders for space propulsion. *Powder Technology*, 270, 46-52. doi: 10.1016/j.powtec.2014.09.048

- Orlandi, O.; Guery, J.F; Lacroix,G.; Chevalier,S.; Desgardin,N. (2005). *HTPB/AP/AL Solid Propellants with Nanometric Aluminum*. Paper presented at the European Conference for Aerospace Sciences (EUCASS), Moscow.
- Osborne, D. T.; & Pantoya, M. L. (2007). Effect of Al Particle Size on the Thermal Degradation of Al/Teflon Mixtures. *Combustion Science and Technology*, 179(8), 1467-1480. doi: 10.1080/00102200601182333
- Poehlein, S. K.; Shortridge, R.G; and Wilham,C.K. (2001). *A Comparative Study of Ultrafine Aluminum in Pyrotechnic Formulations*. Paper presented at the 28th International Pyrotechnics Seminar Proceedings.
- Santhanam, P. R.; & Dreizin., E.L. (2012). Predicting conditions for scaled-up manufacturing of materials prepared by ball milling. *Powder Technology*(221), 403-411.
- Sippel, T. R.; Son, S. F.; & Groven, L. J. (2013a). Altering Reactivity of Aluminum with Selective Inclusion of Polytetrafluoroethylene through Mechanical Activation. *Propellants, Explosives, Pyrotechnics*, 38(2), 286-295. doi: 10.1002/prop.201200102
- Sippel, T. R.; Son, S. F.; & Groven, L. J. (2013b). *Solid Propellant Combustion Enhancement Using Fluorocarbon Inclusions Modified Aluminum* Paper presented at the 8th U.S. National Combustion Meeting University of Utah.
- Sippel, T. R., Son, S. F., & Groven, L. J. (2014). Aluminum agglomeration reduction in a composite propellant using tailored Al/PTFE particles. *Combustion and Flame*, 161(1), 311-321. doi: 10.1016/j.combustflame.2013.08.009
- Sutton, G. P.; and Biblarz, O. (2001). *Rocket Propulsion Elements, 7th Edition*: Wiley.
- Williams, R. A., Beloni, E., & Dreizin, E. L. (2012). Ignition of metal powder layers of different thickness by electrostatic discharge. *Journal of Propulsion and Power*, 28(1), 132-139. doi: 10.2514/1.b34231
- Williams, R. A., Patel, J. V., & Dreizin, E. L. (2014). Ignition of fully dense nanocomposite thermite powders by an electric spark. *Journal of Propulsion and Power*, 30(3), 765-774. doi: 10.1016/0304-3886(85)90041-5

Zhang, S.; Shoenitz, M.; Dreizin, E.L. (2012). *Metastable Aluminum-based reactive Composite materials prepared by cryomilling*. Paper presented at the 50th AIAA Aerospace Sciences, Nashville, TN.